XPS and EXAFS Studies of the Reactions of Co(III) Ammine Complexes with GaAs Surfaces

Bruce J. Tufts,[†] Ian L. Abrahams,[‡] Catherine E. Caley,[‡] Sharon R. Lunt,[†] Gordon M. Miskelly,[†] Michael J. Sailor,[†] Patrick G. Santangelo,[†] Nathan S. Lewis,*[,†] A. Lawrence Roe,[‡] and Keith O. Hodgson*[,‡]

Contribution from the Division of Chemistry and Chemical Engineering, California Institute of Technology, Pasadena, California 91125, and the Department of Chemistry, Stanford University, Stanford, California 94305-5080. *Received January 22, 1990*

Abstract: The chemisorption of Co(II) and Co(III) complexes onto GaAs surfaces has been investigated by X-ray photoelectron spectroscopy (XPS), X-ray absorption spectroscopy, and radiotracer techniques. XPS of (100)-oriented n-GaAs single crystals exposed to aqueous (pH >10) $[Co^{III}(NH_3)_5X]^{n+}$ (X = NH_3, Br^-, HO^-) solutions indicated the deposition of a Co(II)-oxo overlayer of approximate stoichiometry $Co(OH)_2$, with a coverage of (0.2–2.4) × 10^{-8} mol of Co/cm^2 projected area of GaAs. The reaction stoichiometry between Co(III) and GaAs was confirmed by quantitative chemical and X-ray fluorescence analysis, as well as by XPS analysis. X-ray absorption spectroscopy indicated that the oxidation state of the adsorbed Co (from either Co(III) or Co(II) complexes) from aqueous pH = 12 electrolytes was Co(II). Extended X-ray absorption fine structure (EXAFS) spectroscopy at 298 K in contact with aqueous 0.010 M KOH indicated that the Co had (6 ± 1) O or N scatterers at (2.08 ± 0.05) Å and (7 ± 1) Co (or possibly Ga or As) scatterers at (3.13 ± 0.05) Å. EXAFS and XPS methods also indicated that exposure of the Co-GaAs surfaces to 1.0 M KOH–0.8 M Se^{2-}–0.1 M Se_2^{2-} for photoelectrochemical measurements yielded a new Co surface phase, with an approximate composition of $CoSe_{1.8}$.

Introduction

Although chemical modification of semiconductor surfaces can have a major impact on the behavior of photoelectrochemical cells, advanced optoelectronic devices, and chemical sensors,[1-3] at present there is no information concerning the chemical state of any bound metal complex at a semiconductor surface. Key systems of importance in this area include the chemisorption of $RuCl_3 \cdot xH_2O$ to GaAs surfaces,[4] the binding of amines and olefins to CdSe and CdS surfaces,[5] the coating of GaAs with $Na_2S \cdot 9H_2O$,[6] and the reaction of WSe_2 with phosphines.[7] All of these treatments have yielded improved electrical surface properties, and several have resulted in large improvements in the efficiency of photoelectrochemical devices. However, spectroscopic and structural data on these types of systems will be necessary if one is to gain an improved understanding of the chemistry of the surface electrical trap sites.

We have recently demonstrated that group VIIIB coordination complexes provide an excellent system for elucidating the chemical reactivity of GaAs surfaces.[8] Complexes such as $[M^{III}(NH_3)_5X]^{n+}$ (M = Co, Rh, Ir, Ru; X = NH_3, N_3^-, Cl^-, Br^-, H_2O, pyr) have been shown to adsorb onto GaAs electrode surfaces; furthermore, these treatments have been shown to yield extremely high (14–16%) solar-to-electrical energy conversion efficiencies in n-GaAs/KOH-$Se^{-/2-}$ photoelectrochemical cells.[8,9] Questions of interest concern the oxidation state and ligand environment of the bound metal ion, the mechanism of metal ion coordination, the nature of the surface ligating atoms, and the quantity of adsorbed metal. Also of concern are possible changes in chemical state that may occur when, in order to monitor the photoelectrochemical behavior of the surface, the GaAs/(M) surface is exposed to an aqueous 1.0 M KOH–0.8 M Se^{2-}–0.1 M Se_2^{2-} solution. To address these issues, we have performed an X-ray photoelectron spectroscopic (XPS) and X-ray absorption study of the binding of Co(III) ammine complexes to the etched (100) GaAs surface. The XPS measurements have provided oxidation state and coverage information on the surface-bound metal ions, while the extended X-ray absorption fine structure (EXAFS) measurements have provided in situ characterization of the coordination sphere of the metal complex bound onto the semiconductor electrode surface.

* Author to whom correspondence should be addressed.
[†] California Institute of Technology; this work is contribution No. 8074 from the division of Chemistry and Chemical Engineering.
[‡] Stanford University.

Experimental Section

A. Chemicals. All solvents and etches were either J. T. Baker MOS grade or Mallinckrodt Transistar stock. A Barnstead NANOpure water purifier provided 18 MΩ deionized water. All solutions were deaerated by sparging with a stream of dry N_2 gas for at least 15 min.

For X-ray fluorescence (XRF) experiments, As and Ga standards were made from atomic absorption standards supplied by Aldrich, with KBr (Mallinckrodt) used as an internal XRF standard. 1,10-Phenanthroline (phen), 2,2′-bipyridine (bpy), and the buffer agents CAPS (pH = 10.6; 3-(cyclohexylamino)-1-propanesulfonic acid), HEPES (pH = 7.4; 4-(2-hydroxyethyl)-1-piperazineethanesulfonic acid), and MES (pH = 6.15; 4-morpholineethanesulfonic acid) were supplied by Aldrich. Phosphate based pH = 7.0 buffer was obtained from VWR. Hydroxylamine hydrochloride was obtained from J. T. Baker.

The chloride and bromide salts of $[Co^{III}(NH_3)_5X]^{n+}$ (X = N_3^-, NH_3, OH_2, Br^-),[10,11] $[Co^{III}(bpy)_3]^{3+}$,[12] $[Co^{II}(bpy)_3]^{2+}$,[12] and tris(1,10-

(1) Wrighton, M. S. *Acc. Chem. Res.* **1979**, *12*, 303.
(2) Heller, A. In *Photoeffects at Semiconductor-Electrolyte Interfaces*; Nozik, A., Ed.; ACS Symposium Series 146; American Chemical Society: Washington, DC, 1981; pp 57–77.
(3) (a) Parce, J. W.; Owicki, J. C.; Kercso, K. M.; Sigal, G. B.; Wada, H. G.; Muir, V. C.; Bousse, L. J.; Ross, K. L.; Sikic, B. I.; McConnell, H. M. *Science (Washington, D.C.)* **1989**, *246*, 243. (b) Lisensky, G. C.; Meyer, G. J.; Ellis, A. B. *Anal. Chem.* **1988**, *60*, 2531. (c) Madou, M. J.; Morrison, S. R. *Chemical Sensing with Solid State Devices*; Academic Press: San Diego, 1989.
(4) Parkinson, B. A.; Heller, A.; Miller, B. *J. Electrochem. Soc.* **1979**, *126*, 954.
(5) (a) Meyer, G. J.; Leung, L. K.; Yu, J. C.; Lisensky, G. C.; Ellis, A. B. *J. Am. Chem. Soc.* **1989**, *111*, 5146. (b) Meyer, G. J.; Lisensky, G. C.; Ellis, A. B. *J. Am. Chem. Soc.* **1988**, *110*, 4914. (c) Dannhauser, T.; O'Niel, M.; Johansson, K.; Whitten, D.; McLendon, G. *J. Phys. Chem.* **1986**, *90*, 6074.
(6) (a) Sandroff, C. J.; Nottenburg, R. N.; Bischoff, J.-C.; Bhat, R. *Appl. Phys. Lett.* **1987**, *51*, 33. (b) Yablonovitch, E.; Sandroff, C. J.; Bhat, R.; Gmitter, T. G. *Appl. Phys. Lett.* **1987**, *51*, 439. (c) Sandroff, C. J.; Hegde, M. S.; Farrow, L. A.; Chang, C. C.; Harbison, J. P. *Appl. Phys. Lett.* **1989**, *54*, 362.
(7) Parkinson, B. A.; Furtak, T. E.; Canfield, D.; Kam, K.-K.; Kline, G. *Faraday Discuss. Chem. Soc.* **1981**, *70*, 234.
(8) (a) Abrahams, I. L.; Tufts, B. J.; Lewis, N. S. *J. Am. Chem. Soc.* **1987**, *109*, 3472. (b) Abrahams, I. L.; Casagrande, L. G.; Rosenblum, M. D.; Rosenbluth, M. L.; Santangelo, P. G.; Tufts, B. J.; Lewis, N. S. *Nouv. J. Chim.* **1987**, *11*, 157.
(9) Tufts, B. J.; Abrahams, I. L.; Santangelo, P. G.; Ryba, G. N.; Casagrande, L. G.; Lewis, N. S. *Nature (London)* **1987**, *326*, 861.
(10) Literature preparation of $[Co^{III}(NH_3)_6](Cl)_3$: Bjerrum, J.; McReynolds, J. P. *Inorg. Synth.* **1946**, *2*, 217.
(11) Literature preparation—(a) $[Co^{III}(NH_3)_5Cl](Cl)_2$: Schlessinger, G. *Inorg. Synth.* **1967**, *9*, 160. (b) $[Co^{III}(NH_3)_5Br](Br)_2$ and $[Co^{III}(NH_3)_5(OH_2)](Br)_2$: Diehl, H.; Clark, H.; Willard, H. H. *Inorg. Synth.* **1939**, *1*, 186. (c) $[Co^{III}(NH_3)_5(N_3)](Cl)_2$: Linhard, M.; Flygare, H. *Z. Anorg. Chem.* **1950**, *262*, 328.

0002-7863/90/1512-5123$02.50/0

phenanthroline)iron(II)[13] ($[Fe(II)(phen)_3]^{2+}$) were prepared as described in the literature. The perchlorate salts of the above complexes were made by dissolving a small amount (0.5–1.0 g) of the halide salt in a minimum amount of hot (60–70 °C) water, and then adding concentrated perchloric acid dropwise to effect precipitation of the complex with perchlorate as the counterion. The resulting solids were rinsed with 1.0 M perchloric acid on a Büchner funnel until no chloride was observed by a silver ion test and then were washed with cold water and stored in a desiccator. The nitrate salt of $[Co^{III}(NH_3)_5(OH_2)](NO_3)_3$ was made in a similar fashion. $CoCl_2 \cdot 6H_2O$, $CoSO_4 \cdot 6H_2O$, $FeSO_4 \cdot 7H_2O$, and $FeCl_3$ were used as received from J. T. Baker. $[Co^{II}(OH_2)_6](ClO_4)_2$ was obtained from GFS chemicals. All water-soluble cobalt ammine complexes were recrystallized twice from hot water and were characterized by their electronic absorption spectra. We encountered no hazards from manipulation of the perchlorate salts used in this work.

Model compounds *roseo*-$Co(OH)_2$[14] and $CoO(OH)$[15a] were prepared as described previously. $CoSe_2$ was obtained by reacting stoichiometric amounts of powdered Co and Se (1:2 mol ratio) in evacuated ($\approx 10^{-4}$ Torr) sealed quartz tubes held at either 600 or 800 °C for 164 h.[16] A mineralogical sample of $CoAs_3$, Skutterudite (Joint Council on Powder Diffraction Standards: JCPDS No. 10-328),[17] was provided by the Stanford Geology department. CoSe was purchased from Alfa, Inc. All of these model compounds were characterized by their powder X-ray diffraction patterns, which were obtained on either a Scintag Pad-V or a Rigaku Geigerflex XRD-131 powder X-ray diffractometer.

For use in EXAFS studies, the model compounds $Co(OH)_2$, $CoO(OH)$, $[Co^{II}(OH_2)_6](ClO_4)_2$, $CoSe_2$, and $CoAs_3$ were ground to fine powders with an agate mortar and pestle in an N_2-purged glove bag. They were then suspended in a dry boron nitride (Alfa) powder matrix to a 1–3 vol % dilution level.

B. GaAs Surfaces and Electrodes. Preparation of the GaAs electrodes and the 1.0 M KOH–0.8 M K_2Se–0.1 M K_2Se_2 electrolyte and descriptions of the electrode etching procedures, electrochemical cells, and equipment used to record current–voltage parameters have been described elsewhere.[18]

Single crystals of (100)-oriented n-GaAs were grown by organometallic vapor-phase epitaxy to yield $N_D = 2 \times 10^{17}$ cm^{-3} Se doped epilayers or were Czochralski grown to yield $N_D = 1\text{–}4 \times 10^{17}$ cm^{-3} Si doped bulk samples. High surface area GaAs powder was made by grinding 99.9999+% GaAs chunks (Aesar) under an N_2 atmosphere (Vac Atmospheres drybox) in a ball mill or in a mortar. The fraction of powder that passed a 240-mesh sieve (Scienceware) was then retained for further use.

Typical single-crystal samples for XPS experiments were initially cleaved to ca. 1 × 1 cm pieces, degreased by sequential rinsing in trichloroethylene, acetone, and methanol, and then blown dry with N_2. Degreased samples were etched in 4:1:1 (vol) concentrated H_2SO_4:30% H_2O_2:H_2O, rinsed with H_2O, dried with N_2, and passed into an N_2-purged glovebag. In order to strip any GaAs oxides formed during transfer, these pieces were then immersed in deaerated 14.8 M NH_4OH(aq) solution for 30 s, rinsed with deionized water, and dried in N_2. These specimens were then exposed for 1 min to 10-mL aqueous solutions of the desired pH containing 10 mM of either $[Co^{III}(NH_3)_6](Cl)_3$, $[Co^{III}(NH_3)_6](Br)_3$, $[Co^{III}(NH_3)_6](ClO_4)_3$, $[Co^{III}(NH_3)_5OH_2](NO_3)_3$, $[Co^{III}(NH_3)_5Br](Br)_2$, $[Co^{III}(NH_3)_5(N_3)](Cl)_2$, $[Co^{II}(OH_2)_6](ClO_4)_2$, or $[Co^{II}(OH_2)_6](Cl)_2$. Experiments employing $[Co^{II}(OH_2)_6](ClO_4)_2$ in base were performed by first emersing the GaAs sample into neutral solutions of the complex and then adjusting the pH to the desired value by addition of aqueous KOH. The treated samples were then lightly (3–4 mL) rinsed with 18 MΩ water and blown dry with a stream of N_2. Co solutions were made up over a range (1.0–12.9) of pH values. Treated GaAs pieces were then mounted on an XPS sample stub and sealed in air-tight vials for transport to the spectrometer.

To eliminate the possibility of photoreactions of the GaAs or the Co(III) complexes, several GaAs samples were exposed to $[Co^{III}(NH_3)_5X]^{n+}$ (X = NH_3, Br^-, OH_2) solutions in the absence of room light. These samples displayed spectroscopic and electrochemical behavior that was identical with samples that had been manipulated in ambient room light.

Powders of GaAs were treated in a similar fashion. In a glovebag, portions of GaAs powder (ca. 100 mg) were added to 10 mL of the Co(III) and Co(II) solutions (vide supra) for 5 or 10 min. The solid suspensions were then filtered, and the filtrate was analyzed by XRF or UV–vis methods, and the collected solids were rinsed with H_2O and CH_3OH and then dried with N_2 under suction. Depending upon the pH of the Co complex ion solution, this procedure led to a loading of the powders with up to 4% (by weight) Co. Treated powdered samples intended for XPS studies were pressed into a sample of In foil (Alfa) that was molded onto the top of an XPS sample mount.

To investigate potential chemical reactions in the electrochemical solutions of interest, parallel sets of Co-ion treated GaAs powders or single crystals were subsequently exposed to 5-mL solutions of 1.0 M KOH–0.8 M K_2Se–0.1 M K_2Se_2 for 1 min. The samples were then rinsed, dried, mounted as described above, and subjected to XPS analysis.

C. ^{57}Co Studies. γ-Active $^{57}CoCl_2 \cdot 6OH_2$ (2 mCi) was purchased from ICN Chemicals and used to synthesize[10] a 3.46 mM solution (as determined by UV–vis spectrophotometry) of ^{57}Co-enriched $[Co^{III}(NH_3)_6](Cl)_3$. The activity of the final stock solution of the complex was 34.0 $\mu Ci \cdot mL^{-1}$. In the same manner as above, ca. 1-cm^2 pieces of (100) n-GaAs were exposed, in air, to 2.00 mL of the ^{57}Co-enriched stock solution at pH = 1.0 (HCl) or 12.0 (KOH). These GaAs samples were then either immersed in pH = 1.0 (HCl) solution for 30 s and the acid solution assayed for ^{57}Co or etched in 5.00 mL of 4:1:1 (vol) concentrated H_2SO_4:30% H_2O_2:H_2O for 10 s and then rinsed with H_2O. In the latter procedure, care was taken to collect the rinse water into the etch solution. The etch solution and rinse water were then analyzed for γ-activity. Counting was done with a Beckman Model 8000 γ-ray scintillation counter. Standards were prepared from known concentrations of the ^{57}Co-enriched $[Co^{III}(NH_3)_6](Cl)_3$ solution and were used to calibrate the counts observed from the Co-treated GaAs samples. No activity above detectability limits (signal to background 2:1; $\leq 3 \times 10^{-11}$ mol(Co)·cm^{-2}(GaAs)) was observed from etch solutions of untreated GaAs or from ^{57}Co-exposed GaAs that was deliberately etched prior to the ^{57}Co analysis described above.

D. XPS. i. Experimental Procedures. X-ray photoelectron spectra were obtained on a Vacuum Generators Mark II ESCALAB. All spectra were acquired at a base pressure of $<10^{-10}$ Torr with use of nonmonochromatic Al Kα ($h\nu$ = 1486.6 eV) irradiation. The X-ray source was typically operated at 20 mA and 12.5 kV.

A Ag stub was used to determine the instrumental line width, which was observed to be 1.1 eV in narrow scan mode from the full width at half maximum (fwhm) of the Ag 3d doublet peaks at 367.9 and 373.9 binding energy (BeV). All corrected binding energies in this work were referenced to the C 1s line of adventitious carbon at 284.6 BeV. Peak deconvolution was performed with standard software routines provided by Vacuum Generators. Oxidized GaAs substrates showed interference between the Ga 3d and O 2s lines, often precluding reliable calculation of stoichiometric ratios relative to Ga.

Unless otherwise noted, all samples were prepared and mounted on sample stubs under a N_2 atmosphere (in a glovebag) and were transported to the XPS instrument in sealed, gas tight, vials. Total exposure to ambient during transfer to the instrument's N_2-purged fast entry lock was less than 10 s. Etched GaAs that was exposed only to 1.0 M KOH or to pH = 11.0, 0.05 M $KClO_4$ solutions displayed peaks for lattice As 3d at (41.3 ± 0.5) BeV and lattice Ga 3d at (19.4 ± 0.5) BeV and had oxide region peak intensities consistent with $<3 \times 10^{-10}$ mol/cm^2 (i.e., <1/2 monolayer) of arsenic oxides and of gallium oxides (cf. Figure 3). These low background values required careful anaerobic handling of the GaAs through all etching steps and subsequent solution manipulations; however, under these conditions, the appearance of large Ga or As oxide-based XPS signals reliably indicated exposure of the GaAs to additional oxidants (i.e., the Co(III) complexes).

ii. Data Analysis. Estimates of the Co 2p photoelectron escape depth (λ) were obtained by using the method of Seah and Dench,[19] with photoelectron differential cross-sections as given by Scofield.[20] The local environment about Co(II) was assumed to be similar to that of $Co(OH)_2$. This yielded a value of λ_{Co2p} = 18 Å. Employing the simple homogeneous

(12) (a) Blau, F. *Monatsh. Chem.* **1889**, *10*, 372. (b) Blau, F. *Monatsh. Chem.* **1898**, *19*, 647. (c) Burstal, F. M.; Nyholm, R. S. *J. Chem. Soc.* **1952**, 3570.

(13) (a) Blau, F. *Monatsh. Chem.* **1898**, *19*, 669. (b) Shilts, A. A. *J. Am. Chem. Soc.* **1960**, *82*, 3000.

(14) Brauer, G. *Handbook of Preparative Inorganic Chemistry*, 2nd ed.; Academic Press: New York, 1965; Vol. 2, p 1521.

(15) (a) Feitknecht, W.; Bēdert, W. *Helv. Chim. Acta* **1941**, *24*, 683. (b) Delaplane, R. G.; Ibers, J. A.; Ferraro, J. R.; Rush, J. J. *J. Chem. Phys.* **1969**, *50*, 1920.

(16) (a) Heide, H. van der; Hemmel, R.; Bruggen, C. F. van; Haas, C. *J. Solid State Chem.* **1980**, *33*, 17. (b) Ramdohr, P.; Schmitt, M. *Neues Jahrb. Mineral. Monatsh.* **1955**, *6*, 133. (c) Bohm, F.; Gronvold, F.; Haraldsen, H.; Prydz, H. *Acta Chem. Scan.* **1955**, *9*, 1510.

(17) Mandel, N.; Donohue, J. *Acta Crystallogr. Sect. B: Struct. Sci.* **1971**, *B27*, 2288.

(18) (a) Gronet, C. M.; Lewis, N. S. *J. Phys. Chem.* **1984**, *88*, 1310. (b) Tufts, B. J.; Abrahams, I. L.; Casagrande, L. G.; Lewis, N. S. *J. Phys. Chem.* **1989**, *93*, 3260. (c) Lunt, S. R.; Casagrande, L. G.; Tufts, B. J.; Lewis, N. S. *J. Phys. Chem.* **1988**, *92*, 5766.

(19) Seah, M. P.; Dench, W. A. *Surf. Interface Anal.* **1979**, *1*, 2.

(20) Scofield, J. H. *J. Electron Spectrosc. Relat. Phenom.* **1976**, *8*, 129.

overlayer model of photoelectron attenuation,[21] the surface coverage was then determined with respect to the intensity, photoelectron escape depth (λ_{As3d} = 25 Å), molar density (n_{As} = 3.68 × 10^{-2} mol·cm^{-3}) for As in the substrate GaAs, the integrated Co $2p_{3/2}$ peak intensity, the known values of the sample-detector angle, and the atomic number density (3.87 × 10^{-2} mol·cm^{-3}) for Co in $Co(OH)_2$.[22]

In calculating the coverages of As_2O_3, we assumed the molar density of vitreous arsenic oxide (ρ = 1.89 × 10^{-2} mol·cm^{-3})[23] and used the value of λ calculated from the method of Seah and Dench[19] as λ_{As3d} = 36 Å. For gallium oxide, the average of the molar densities of the α and the β phases, ρ = 3.30 × 10^{-2} mol·cm^{-3},[24] was used (method of Seah and Dench)[19] to yield an escape depth of λ_{Ga3d} = 28 Å. XPS signals from the C 1s region showed that more than one type of hydrocarbon was in the surface overlayer. We therefore estimated the value of the hydrocarbon molar density as ρ = 1.5 × 10^{-2} mol (C)·cm^{-3} and the carbon atomic number density as ρ = 3.3 × 10^{-2} g-atom·cm^{-3} and used the experimentally determined value[25] of λ = 35 Å for the mean free path of the photoelectrons in the organic film.

Surface morphology and relative stoichiometry were obtained by comparison of XPS peak intensities between the substrate As 3d or Ga 3d lines, the O 1s line, and the Co 2p lines on (100)-oriented n-GaAs over a range of sample-detector angles.[26] The simple XPS substrate/overlayer intensity model of Fadley[27] was applied, assuming that substrate oxides were closest to the GaAs interface, followed by a cobalt–oxo or –seleno layer, and finally an adventitious hydrocarbon layer. In determining the stoichiometric ratio of Co:O in the overlayer, a correction for sources of O other than $Co(OH)_2$ was made to the raw O 1s intensity. The sources were clearly identified from their peak positions: the oxides of GaAs ($\lambda_{O1s}(As_2O_3)$ = 29 Å and $\lambda_{O1s}(Ga_2O_3)$ = 22 Å), signals for carboxy-*O* in the C 1s region at ≥286 BeV (λ_{O1s}(C–*O*) = 37 Å), and those for H_2O in the O 1s region at ≥534 BeV ($\lambda_{O1s}(H_2O)$ = 22 Å). The λ_{O1s} escape depths were estimated from the method of Seah and Dench.[19] Assuming an atomic O density ρ = 2.8 × 10^{-2} g-atom·cm^{-3} for carboxy-*O* and ρ = 5.6 × 10^{-2} g-atom·cm^{-3} for H_2O, a background O 1s intensity was determined and subtracted from the raw O 1s signal. Deviations from the expected stoichiometric ratios were interpreted as evidence of a non-uniform surface phase.[28] We have assumed that a non-uniform surface phase may be modeled as a void filled thin film, the density of which varies in the direction normal to the surface.

For those GaAs samples subsequently exposed to $Se^{-/2-}$ electrolyte, estimates of Co coverage were based on the integrated Co $3p_{3/2}$ and $3p_{1/2}$ intensities (the two core levels give rise to a single line in the XPS spectrum).[29] The Co 3p and Se 3d lines were used to derive a stoichiometric relationship between Co and Se because these lines are only 4 eV apart in binding energy. The closeness of the lines minimizes the systematic error due to differences in the spectrometer transmission response as a function of photoelectron energy. Following the procedure described above, using the atomic density of Co in Trogtalyte, $CoSe_2$ (ρ = 3.3 × 10^{-2} g-atom·cm^{-3}),[16bc] we obtained electron escape depths of λ_{Co3p} = 20 Å and λ_{Se3d} = 20 Å.

E. EXAFS. Cobalt K edge EXAFS spectra were obtained on beam lines II-3, IV-2 (unfocussed), and VII-3 at the Stanford Synchrotron Radiation Laboratory (SSRL). Synchrotron radiation (derived from a ring electron current of 30–80 mA and ca. 3.0 GeV energy) was passed through a scanning Si (220) double-crystal monochromator prior to sample illumination. EXAFS data on the model compounds were obtained under 10^{-6} Torr at 10 K in the transmission mode. These data were collected from ca. 7400 eV, through the Co K edge of our internal calibration Co foil at 7709.30 eV, to ca. 8800 eV with N_2 ionization detectors. EXAFS data for Co treated GaAs powders were collected under 10^{-6} Torr at 10, 77, and 298 K by monitoring the fluorescence lines of Co $K\alpha_{1,2}$ at 6930 and 6915 eV with an ionization-type fluorescence detector[30ab] and an Fe sheet high pass filter supplied by the SSRL Biotechnology group.

Absorbance (or fluorescence) vs wavelength data were collected in 20–30-min scans, with several scans collected and averaged to improve the signal-to-noise ratio. Derivative spectra of the edge region contained several small inflection points; we therefore took the energy at half-height of the absorption jump as the edge position. Bond distances and the number of scatterers were calculated by fitting the oscillatory part of the EXAFS spectra to the EXAFS equation,[30c–f] using phase factors and scattering amplitudes determined experimentally from the model compounds. The average Co–O distance in $[Co^{II}(OH_2)_6](ClO_4)_2$ was taken as the average Co–O distance from the crystallographically determined Co–O bond lengths in $[Co^{II}(OH_2)_6](NH_4SO_4)_2$,[31a] $[Co^{II}(OH_2)_6(NO_3)_2$,[31b] and $[Co^{II}(OH_2)_6](SiF_6)$.[31c]

Immediately before data collection, either a cobalt model compound/BN powder blend or a Co ion treated GaAs powder was pressed into a sample holder that was fashioned from a 3 × 25 mm slot cut through a 3 mm thick Cu plate. The powder sample was sealed in place with Kapton tape. The loaded sample holder was mounted onto the cold head of an Air Products Displex 10 K closed cycle He gas refrigerator or of a home-made liquid nitrogen cooled cold finger. This sample assembly was evacuated to $\leq 10^{-6}$ Torr before data collection was initiated. Kapton film (1–2 mil) was used as the refrigerator window material to allow for X-ray excitation and for detection of both transmission (BN matrix) and fluorescence (GaAs powder) EXAFS spectra.

F. Quantitative Chemical Analysis. Aluminum foil wrapped vials were charged with freshly ground GaAs (10–20-mg fraction passing a 240-mesh sieve) and stoppered in the glovebox. Standard syringe techniques were used to transfer ca. 6 mL of deaerated 5.0 mM $[Co^{III}(NH_3)_6]^{3+}$ solutions at either 0.10 M HCl (pH = 1.0), 50 mM HEPES (pH = 7.4), 50 mM CAPS (pH = 10.6), or 14.8 M NH_4OH (pH = 12.9) to one set of vials. Another set of vials charged with GaAs was treated with the various pH solutions containing no Co complex. At least three vials were used for each combination of blank and Co complex at each pH. A parallel set of trials at 0.10 M HCl was carried out with Fe^{3+}, from ferric chloride, in place of the Co(III) complex.

Reaction vials were stored in the dark for 15–24 h and typically were stirred for 6–8 h. At the end of the reaction period, the sample was analyzed under N_2 for Co(II) ion, by removing an aliquot of the reaction solution via gas tight syringe and converting any Co(II) ions in the analyte to the Co(II) thiocyanate complex via a slightly modified method.[32] In place of acetylacetone, we used a (2:5) mixture of water:acetone in the final analyte solution to form the cobalt complex. Cobalt(II) thiocyanate (λ_{max} = 622 nm) was spectrophotometrically detected[32] with a Hewlett-Packard (HP) 8452A diode array UV–vis spectrophotometer. A series of calibration curves, determined for a range of Co(III) and Co(II) concentrations (4.3 × 10^{-5} to 2.50 × 10^{-3} M) at each pH, was used to convert measured absorbances to initial reactant concentrations. The limits of detectability of the HP UV–vis made it possible to monitor both Co(II) and Co(III) complex ions simultaneously, down to concentrations of 30 and 150 μM, respectively. The GaAs-driven conversion of Fe^{3+} to Fe^{2+} at 0.10 M HCl was monitored by converting any iron(II) aquo ions to the tris(phenanthroline)iron(II) complex. The oxidation state and concentration of the resulting Fe complex were observed by UV–vis spectrophotometry. The UV–vis detectability limit for the Fe(II) complex was 30 μM.

Product As and Ga ions formed in the reaction solution were determined by X-ray fluorescence (XRF) analysis. Both arsenic (III) and gallium (III) oxides are amphoteric, and therefore are soluble at either low or high pH conditions.[33] We did not observe solubility product limited concentrations of arsenic (III) or gallium (III) ions, up to and including the maximum observed values of ca. 1 mM. Using anaerobic

(21) Feldman, L. C.; Mayer, J. W. *Fundamentals of Surface and Thin Film Analysis*; North-Holland: New York, 1986.

(22) The molar density was calculated from the formula weight and mass density as reported in the following: Weast, R. C., Astle, M. J., Eds. *CRC Handbook of Chemistry and Physics*; Chemical Rubber Co.: Boca Raton, 1980; Vol. 60, p B-73. The atomic number density of an atom in a compound is given by the mass density of the compound multiplied by the stoichiometric coefficient for the atom.

(23) Weast, R. C., Astle, M. J., Eds. *CRC Handbook of Chemistry and Physics*; Chemical Rubber Co.: Boca Raton, 1980; Vol. 60, p B-57.

(24) Weast, R. C., Astle, M. J., Eds. *CRC Handbook of Chemistry and Physics*; Chemical Rubber Co.: Boca Raton, 1980; Vol. 60, p B-80.

(25) Bain, C. D.; Whitesides, G. M. *J. Phys. Chem.* **1989**, *93*, 1670.

(26) The sample-detector angle was varied over the range θ = 0–70°. See Table II.

(27) Fadley, C. S. *Prog. Solid State Chem.* **1976**, *11*, 265.

(28) Phillips, L. V.; Salvati, L.; Carter, W. J.; Hercules, D. M. In *Quantitative Surface Analysis of Materials*; McIntyre, N. S., Ed.; ASTM Special Technical Publication 643; American Society for Testing and Materials: Philadelphia, 1978; pp 47–63.

(29) Kim, K. S. *Phys. Rev. B* **1975**, *11*, 2177.

(30) (a) Stern, E. A.; Heald, S. M. *Rev. Sci. Instr.* **1979**, *50*, 1579. (b) Lytle, F. W.; Greegor, R. B.; Sandstrom, D. R.; Marques, E. C.; Wong, J.; Spiro, C. L.; Huffman, G. P.; Huggins, F. E. *Nucl. Instr. Meth.* **1984**, *226*, 542. (c) Cramer, S. P.; Hodgson, K. O.; Stiefel, E. I.; Newton, W. E. *J. Am. Chem. Soc.* **1978**, *100*, 2748. (d) Cramer, S. P.; Hodgson, K. O. *Prog. Inorg. Chem.* **1979**, *15*, 1. (e) Scott, R. A.; Hahn, J. E.; Doniach, S.; Freeman, H. C.; Hodgson, K. O. *J. Am. Chem. Soc.* **1982**, *104*, 5364. (f) Scott, R. A. *Methods Enzymol.* **1985**, *117*, 414.

(31) (a) Prelesnik, B. V.; Gabela, F.; Ribár, B.; Krstanovic, I. *Cryst. Struct. Commun.* **1973**, *2*, 581. (b) Chastain, R. V.; Natt, J. J.; Witkowska, A. M.; Lingafelter, E. C. *Acta Crystallogr.* **1967**, *22*, 775. (c) Ray, S.; Zalkin, A.; Templeton, D. H. *Acta Crystallogr. Sect. B: Struct. Sci.* **1973**, *B29*, 2741.

(32) Brown, W. B.; Steinbach, J. F. *Anal. Chem.* **1959**, *31*, 1805.

(33) Pourbaix, M. *Atlas of Electrochemical Equilibria in Aqueous Solution*; Pergamon: New York, 1966.

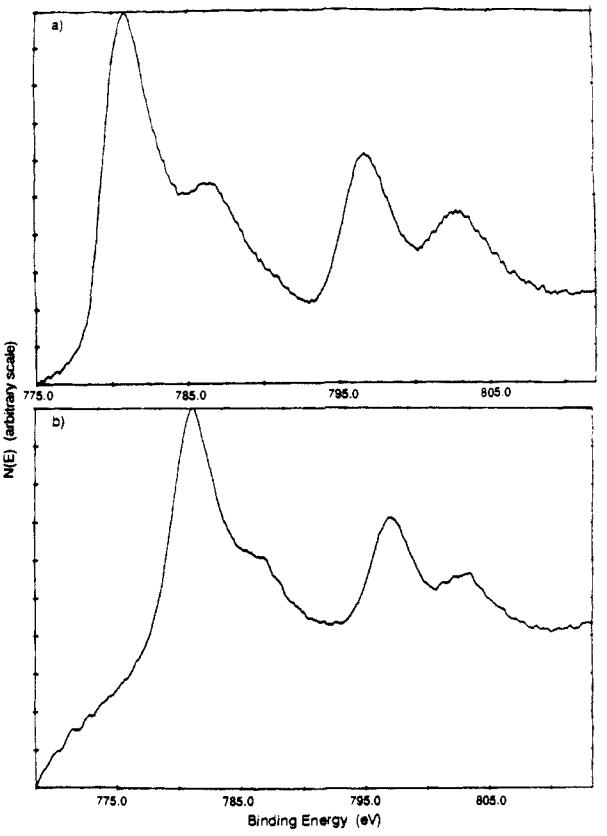

Figure 1. Co 2p region XPS of GaAs samples exposed to basic (pH > 10) aqueous solutions of $[Co^{III}(NH_3)_6]^{3+}$ complex. The raw data are displayed corrected for binding energy relative to C 1s (a) (100)-oriented n-GaAs single-crystal substrate; (b) GaAs powder on In foil.

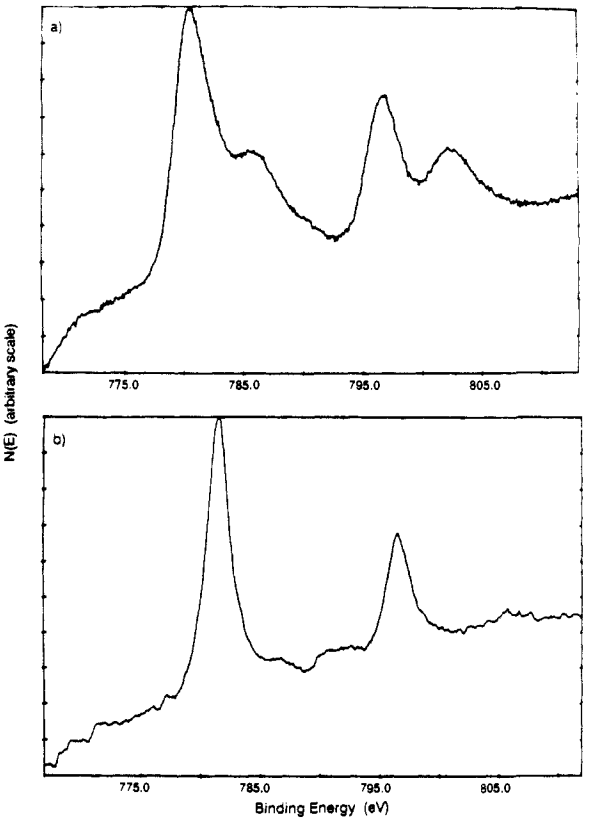

Figure 2. Co 2p region XPS of model compounds; the raw data are displayed corrected for binding energy relative to C 1s (a) *roseo*-$Co(OH)_2$ on In foil; (b) $[Co^{III}(NH_3)_6](Br)_3$ on In foil at T = 180 K.

syringe techniques, a typical reaction solution was filtered (0.2 μm filter) to remove suspended GaAs. A 1.00-mL aliquot of the filtrate was transferred by micropipet to a thin (1 mil) Saran plastic bottomed X-ray fluorescence sample cup to which 30.0 mM KBr solution was added for use as an internal XRF standard. XRF analysis was performed on a KEVEX 0700 XES instrument. Co, Ga, and As ions were probed by X-rays from a Ag target operated at 35 kV and 0.35 mA. Fe ions were detected with a Ge target operated at 20 kV and 0.2 mA. Acquisition times of 300 or 500 s were used to obtain areas from the intensities of the X-ray fluorescence peaks. Employing standard computer deconvolution techniques, the measured intensities were converted to solution concentrations by comparison to intensities obtained from stock solutions of As, Ga, Co, and Fe at known concentrations under identical instrumental conditions. The detectability limits (S/N < 2, ±50% of the detectability limit) using this method were 10, 80, 750, and 840 μM for As, Ga, Co, and Fe, respectively.

Determination of the complete stoichiometry of the redox reaction at pH = 10.6 (CAPS buffer) was not feasible by these techniques. The amount of observed Co(II) ion could not be correlated with the disappearance of Co(III) or with the final As and Ga ion concentrations. In the absence of stabilizing ligands (e.g. NH_3), *roseo*-$Co(OH)_2$ is insoluble (K_{sp} = 1.99 × 10^{-15} M^3) at pH = 10.6,[34] which likely accounts for the irreproducible variations in the [As]:[Ga]:[Co(II)] ratio of soluble ions observed in the XRF experiments at this pH.

The pH stability of a Co-containing surface layer on GaAs was probed by first reacting the $[Co^{III}(NH_3)_6]^{3+}$ complex with GaAs powder in 0.010 M KOH as above, removing the reaction solution, and then subjecting the resulting solids to either 0.10 M HCl, VWR phosphate buffer (pH = 7.0), or 0.010 M KOH solutions for 30 s. The resulting solution was then syringe filtered (0.45 μm) and any Co(II) in the analyte was converted to the cobalt(II) thiocyanate complex (vide supra) and was determined spectrophotometrically.

Results

1. XPS Studies of Co Chemisorption on GaAs. A. Co(III) Complexes: XPS Spectra in the Co 2p, As 3d, and Ga 3d Regions.

Both single-crystal and powdered GaAs samples were observed to bind Co after exposure to basic 0.010 M KOH aqueous Co(III) ammine solutions. Figure 1 displays the X-ray photoelectron (XP) spectra that were obtained from these samples. The spectra exhibited two primary signals in the Co 2p region (781.1 and 797.0 BeV, relative to adventitious carbon at C 1s = 284.6 BeV) with two satellite peaks (786.2 and 802.8 BeV). A wide scan displayed the expected additional Co XP and Auger lines, but it did not reveal signals corresponding to the presence of N, Cl, or elements other than C, O, Ga, As, and Co. Variation in the identity of the sixth ligand (X = N_3^-, Br^-, OH^-, NH_3) did not produce any change in the XPS spectrum of the Co 2p region, nor did such variation yield any new peaks in the XPS wide scans. Table I summarizes the peak positions obtained for representative samples in this series of XPS experiments.

XPS data were also obtained for several pure Co(II) and Co(III) coordination compounds. *roseo*-$Co(OH)_2$ exhibited parent lines at 780.6 and 796.8 BeV and daughter peaks at 785.6 and 802.5 BeV (Figure 2a). The XPS of $[Co^{III}(NH_3)_6](Br)_3$, cooled to 180 K, produced a spectrum with lines at 781.6 and 796.6 BeV and no satellite structure (Figure 2b). No noticeable photoreduction of Co(III) to Co(II) was observed on this sample. The spectra of these complexes are in agreement with the general expectations of parent peak splittings Δ = 16.1 ± 0.3 eV and satellite structure for high-spin (S = 3/2) Co(II)[35] complexes and parent peak splittings Δ = 15.0 ± 0.3 eV with no satellite structure for low-spin Co(III) compounds.[35]

The peak positions and satellite structure of the Co 2p lines in Figures 1 and 2a, and the similarity to the known XP spectra for Co(II) complexes,[35] indicate that the oxidation state of the GaAs-bound Co is Co(II). This implies that the mechanism of Co(III) binding to the GaAs involves a redox reaction. The loss of XPS signals attributable to either coordinated ammines or other

(34) Feitknecht, W.; Schindler, P. *Pure Appl. Chem.* **1963**, *6*, 130.

(35) (a) Frost, D. C.; McDowell, C. A.; Woolsey, I. S. *Chem. Phys. Lett.* **1972**, *17*, 320. (b) Frost, D. C.; McDowell, C. A.; Woolsey, I. S. *Mol. Phys.* **1974**, *27*, 1473. (c) Haraguchi, H.; Fujiwara, K.; Fuwa, K. *Chem. Lett.* **1975**, 409.

Table I. XPS Peak Positions[a] for Model Compounds and Surface Components of Etched and Reacted GaAs Interfaces

sample	Co 2p parent		Co 2p satellite		N 1s	Br 3d/ Cl 2p	O 1s	Se 3d
$[Co^{III}(NH_3)_6](Br)_3$	781.6 Δ^b = 15.0	796.6			399.7	68.5		
roseo-$Co(OH)_2$	780.6 Δ = 16.2	796.8	785.6 Δ = 16.9	802.5			530.6	
CoSe (sputtered)	777.9 Δ = 14.9 Co 3p line = 58.8	792.8						54.4
(100) GaAs + $[Co^{III}(NH_3)_6](ClO_4)_3$ 0.010 M KOH	781.1 ± 0.5 Δ = 15.9 ± 0.1	797.0 ± 0.4	786.2 ± 0.4 Δ = 16.6 ± 0.3	802.8 ± 0.4	*d*	*d*	531.3 ± 0.5	
(100) GaAs + $[Co^{III}(NH_3)_5(OH)](NO_3)_2$ 0.010 M KOH	780.8 Δ = 16.2	797.0	786.4 Δ = 16.4	802.8	*d*	*d*	531.0	
(100) GaAs + $[Co^{III}(NH_3)_6](ClO_4)_3$ pH = 12.9 (satd NH_3)	(781)[c]	*d*	*d*	*d*	*d*	*d*	532.1	
240 mesh GaAs + $[Co^{III}(NH_3)_5Br](Br)_2$ pH = 11.0	781.0 Δ = 16.1	797.1	786.3 Δ = 16.4	802.7	*d*	*d*	531.0	
240 mesh GaAs + $[Co^{III}(NH_3)_5N_3](Cl)_2$ pH = 10.7	781.6 Δ = 16.0	797.6	787.0 Δ = 16.6	803.6	*d*	*d*	531.3	
(100) GaAs + $[Co^{III}(NH_3)_5N_3](Cl)_2$ pH = 6.2 (MES buffer)	*d*	*d*	*d*	*d*	*d*	*d*	531.9	
(100) GaAs + $[Co^{III}(NH_3)_6](Br)_3$ pH = 2.0	*d*	*d*	*d*	*d*	*d*	*d*	531.7	
(100) GaAs + $[Co^{III}(bpy)_3](ClO_4)_3$ pH = 11.3	(781)[c]	*d*	*d*	*d*	*d*	*d*	531.8 ± 0.1	
(100) GaAs + $[Co^{II}(OH_2)_6](Cl)_2$ 0.010 M KOH	781.1 ± 0.4 Δ = 16.1 ± 0.1	797.2 ± 0.4	786.4 ± 0.4 Δ = 16.5 ± 0.1	802.9 ± 0.4	*d*	*d*	531.0 ± 0.3	
(100) GaAs + $[Co^{II}(OH_2)_6](Cl)_2$ pH = 12.9 (satd NH_3)	(782)[c] Δ = 16	(798)[c]	*d*	*d*	*d*	*d*	532.2	
(100) GaAs + $[Co^{II}(bpy)_3](Cl)_2$ pH = 12.0	(781)[c] Δ = 16	(797[c])	*d*	*d*	*d*	*d*	532.7	
(100) GaAs + $[Co^{III}(NH_3)_6](ClO_4)_3$ (0.010 M KOH) + KOH-$Se^{-/2-}$	778.4 Δ = 14.9 Co 3p line = 59.0	793.3	*d*	*d*		*d*	531.2	54.2 ± 0.3

[a] XPS core lines referenced against C 1s = 284.6 binding eV (BeV). Peak positions from repeated experiments are shown as the mean binding energy ± one standard deviation. [b] Separation between parent lines or between satellite lines. [c] Edge of poorly defined peak barely discernible above background. [d] No peak observed above background.

inner-sphere ligands of $[Co^{III}(NH_3)_5X]^{n+}$ (X = N_3^-, Br^-, HO^-, NH_3) is consistent with the lability of the Co(II) oxidation state[36] and confirms the involvement of electron-transfer steps in the chemisorption of these complexes.

The reduction of Co(III) to Co(II) in 0.010 M KOH solution implies that oxidation of the GaAs should also occur. For exposure to $[Co^{III}(NH_3)_6]^{3+}$, this was confirmed by the presence of an arsenic oxide (As_2O_3) line at 43.6 BeV (As 3d region) and a gallium oxide line at 20.7 BeV (Ga 3d region) (Figure 3). Oxidized Ga and As were also observed after exposure of the GaAs to $[Co^{III}(bpy)_3]^{3+}$, but no detectable ($\leq 2 \times 10^{-10}$ mol·cm^{-2}) oxide was observed after exposure to $[Co^{II}(bpy)_3]^{2+}$ or to $[Co^{II}(NH_3)_6]^{2+}$ in aqueous NH_3 (Table II). Oxidation of the GaAs thus takes place with a variety of Co(III)-based reagents and is detectable by both XPS and chemical analysis for the resulting Co(II) (vide infra).

The lack of detectable Co XPS signal from $[Co^{III/II}(bpy)_3]^{3+/2+}$ exposure at $1 \leq pH \leq 12.0$ (Tables I and II) demonstrates that a simple electrostatic interaction is insufficient to explain the chemisorption process. This is the case even for pH >11, where surface oxides might be expected to generate a substantial concentration of ionized hydroxide-like species. The observed oxidation of the GaAs substrate in the presence of basic solutions of $[Co^{III}(bpy)_3]^{3+}$ does, however, support the involvement of electron-transfer steps in the chemisorption mechanism (Table II).

The chemisorption process also was found to depend on the pH of the aqueous solution. In contrast to the facile chemisorption from $[Co^{III}(NH_3)_5X]^{n+}$ (X = N_3^-, Br^-, OH^-, NH_3) in 0.010 M KOH, we were unable to detect bound Co or oxidation of GaAs using Co(III) ammine complexes at pH = 1–2 (Tables I and II). This is in accord with chemical studies indicating that $[Co^{III}(NH_3)_6]^{3+}$ is not sufficiently oxidizing to react with GaAs in acidic media (vide infra). Notably, the solubility product[34] of *roseo*-$Co(OH)_2$ is $K_{sp} = 1.99 \times 10^{-15}$ M^3, indicating that if a $Co(OH)_2$ species is produced, it would be expected to dissolve at low pH values. However, by XPS, we also observed negligible oxidation of the substrate GaAs in 0.10 M HCl in the presence of $[Co^{III}(NH_3)_5X]^{n+}$ (X = OH_2, Br^-) or at pH = 2.0 in the presence of $[Co^{III}(NH_3)_6]^{3+}$. We thus conclude that no reaction between GaAs and $[Co^{III}(NH_3)_5X]^{n+}$ (X = NH_3, OH_2, Br^-) occurred on our time scale at pH = 1–2.

The proposed redox mechanism also implies that reduction of more than one monolayer equivalent of Co(III) is possible. Quantitative coverage information obtained from an analysis of the XPS peak intensities is summarized in Table II. Four separate experiments using single-crystal (100) n-GaAs surfaces with Co(III) ammine complexes ($11.3 < pH < 12$) yielded Co coverages between $(2.4 \pm 1.0) \times 10^{-9}$ and $(24.0 \pm 3.2) \times 10^{-9}$ mol(Co)/cm^2(GaAs). This corresponds to approximately 2–18 monolayers of $Co(OH)_2$. After corrections for O 1s intensity due to water, substrate oxides, and adventitious oxides of carbon, the expected O_{corr}/Co ratio for $Co(OH)_2$ should be 2.0. This is in excellent agreement with the average experimental value of $O_{corr}/Co = 2.1 \pm 0.2$ (Table II). Arsenic oxide coverages ranged between $(5 \pm 2) \times 10^{-10}$ and $(1.9 \pm 0.1) \times 10^{-9}$ mol/cm^2(GaAs), with As_2O_3/Co mol ratios of 0.12 ± 0.04. For a 6-electron oxidation of GaAs (vide infra),[37] the expected As_2O_3/Co mol ratio is 0.083; this, however, assumes that no As_2O_3 or Co(II) dissolves into the electrolyte. Wet chemical studies of Co loaded GaAs powder (vide infra) have demonstrated that if the pH of the rinse water is sufficiently low ($1.0 < pH < 7.0$) surface-bound $Co(OH)_2$ will dissolve, thus implying that the surface composition will not accurately reflect the reaction stoichiometry at this pH. On

(36) Basolo, F.; Pearson, R. G. *Mechanisms of Inorganic Reactions*, 2nd ed.; Wiley: New York, 1967.

(37) (a) Gerischer, H. *J. Vac. Sci. Technol.* **1979**, *15*, 1422. (b) Memming, R. *J. Electrochem. Soc.* **1978**, *125*, 117.

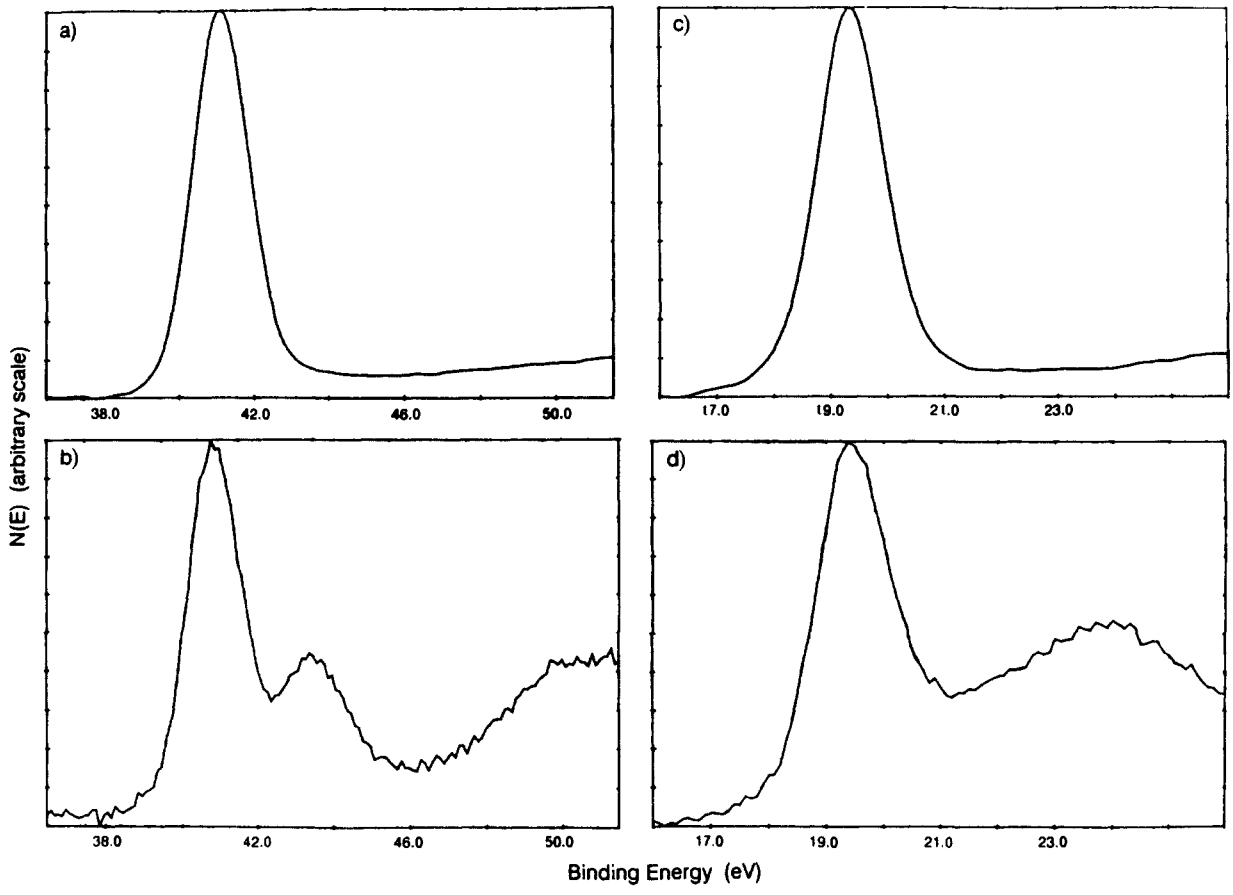

Figure 3. XPS of anaerobically handled (100)-oriented n-GaAs substrates. The raw data are displayed corrected for binding energy relative to C 1s. (a) As 3d region of 4:1:1 (concentrated H_2SO_4:30% H_2O_2:H_2O) etched, base (1.0 M KOH) exposed sample. Sample-normal to detector angle 65°. (b) As 3d region of an etched substrate subsequently exposed to 0.010 M $[Co^{III}(NH_3)_6]^{3+}$ complex at pH = 12. The new peak at ca. 44 BeV is due to As_2O_3. Sample-normal to detector angle 15°. (c) Ga 3d region of the same substrate as in a. (d) Ga 3d region of the same substrate as in b. The presence of Ga_2O_3 (20.7 BeV) has resulted in a broadening of the substrate line toward higher binding energies. Interference from the O 2s line can be seen as a broad peak centered about 24 BeV.

substrates that contained substantial amounts of oxide, it was difficult to monitor the Ga 3d line due to interference from the O 2s line. On those samples where it was possible to monitor gallium oxide peaks, we observed Ga_2O_3/As_2O_3 mol ratios of 0.37 ± 0.05.

Further information on the stoichiometry and morphology of the surface phase was obtained from angle-resolved XPS experiments on single-crystal n-GaAs surfaces (Table II). For a given GaAs sample treated with a basic Co(III) ammine complex, the angular dependence of the XPS intensity deviated from that expected for a homogeneous, fixed thickness, overlayer. The systematic variations in the overlayer/substrate intensity ratios of thin adlayers were consistent with that of a rough, coarse interface. The ratio variations of thicker oxo layers were similar, and they could be viewed as due to a porous oxide layer. Additionally, at increasingly surface sensitive take-off angles, the O/Co ratio also increased. This trend in the O/Co ratio indicated a surface phase that was more oxygen rich at the overlayer/vacuum interface than at the substrate/overlayer interface. The presence of hydrated outermost layers of the cobalt–oxo phase would be consistent with the observed angular dependence of the O/Co ratio. Support for this assignment was obtained from an observed increase in the intensity of the high binding energy side (~534 BeV) of the O 1s XP peak at increasingly surface sensitive take-off angles. This binding energy is typical of surface-bound H_2O.[38]

B. Co(II) Complexes: XPS Studies of Co Chemisorption on GaAs. Cobalt was also observed to adsorb on GaAs that had been exposed to basic aqueous solutions of $[Co^{II}(OH_2)_6]^{2+}$. XP spectra

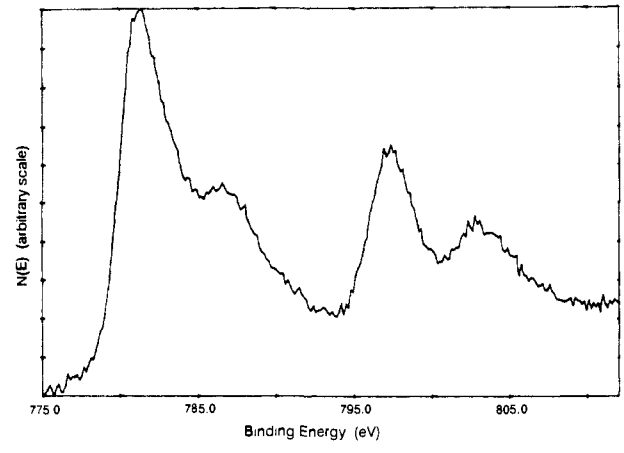

Figure 4. Co 2p region XPS of an etched (100)-oriented n-GaAs substrate exposed to a basic (pH = 12) 0.010 M $[Co^{II}(OH_2)_6](Cl)_2$ solution. The raw data are displayed corrected for binding energy relative to C 1s.

of single-crystal and powdered GaAs samples yielded Co 2p lines at 780.8 and 796.9 BeV and satellite structure at 786.0 and 802.5 BeV, shown in Figure 4. To within 0.2 eV, the primary Co 2p XPS peak positions and splittings observed for GaAs surfaces exposed to $[Co^{II}(OH_2)_6]^{2+}$ (0.010 M KOH) or $[Co(III)(NH_3)_6]^{3+}$ were identical. Additionally, the parent Co 2p peak positions and splitting for Co(II)-treated GaAs were within 0.2 eV of signals obtained from pure *roseo*-$Co(OH)_2$.

Solutions of Co(II) ions made basic by the addition of hydroxide ion quickly formed precipitates of $Co(OH)_2$, and in the presence of GaAs, apparently some of this precipitate nucleated on the

(38) Augustynski, J.; Koudelka, M.; Sanchez, J.; Conway, B. E. *J. Electroanal. Chem.* **1984**, *160*, 233.

Table II. Surface Coverage[a] of Reacted (100) GaAs Interfaces

		GaAs substrate																					
		Ga 3d		As 3d				As_2O_3			Ga_2O_3			Co $2p_{3/2}$			O 1s			Se 3d			C 1s	
sample	θ, deg	peak[c]	int[d]	peak	int	As/Ga[e]	peak	int	coverage[f]	peak	int	coverage[g]	peak	int	$\Gamma_{Co(OH)_2}$[h]	peak	int	O_{corr}/Co[i]	peak	int	Γ_{CoSe_2}[j]	Se/Co[e]	int	Γ_{CHO}[k]
4:1:1 etched GaAs	0	18.9	3897	40.8	3468	0.89	*m*			*m*			*m*			532.3	11660		*n*				*o*	
+ 1.0 M KOH	55	19.0	3727	41.0	3438	0.92	*m*			*m*			*m*			532.4	11420		*n*				3561	2.2×10^{-9}
$T \approx 180$ K[l]																							
4:1:1:1 etched GaAs	0	19.8	2288	41.7	2000	0.87	*m*			*m*			*n*			532.8	7961		*n*				6186	7.5×10^{-9}
+ $KClO_4$, pH = 11.0	55	19.9	1815	41.8	1743	0.96	*m*			*m*			*n*			532.6	9340		*n*				7842	5.2×10^{-9}
room temp (RT)																							
GaAs + $[Co^{III}(NH_3)_6]^{3+}$	10	19.0	1933	41.1	1654	0.86	43.7	130	5×10^{-10}	20.6	36	2×10^{-10}	781.3	1387	4.4×10^{-9}	531.5	13934	2.00	*n*				5444	5.1×10^{-9}
0.010 M KOH	30	*n*		41.0	1472		43.6	180	7×10^{-10}	*n*			781.1	1715	4.4×10^{-9}	*n*			*n*				*n*	
$T \approx 180$ K	55	*n*		41.1	753		43.7	105	5×10^{-10}	*n*			781.3	1557	4.3×10^{-9}	*n*			*n*				*n*	
	70	19.1	910	41.1	882	0.97	43.7	124	3×10^{-10}	20.8	25	1×10^{-10}	781.3	1696	2.4×10^{-9}	531.6	13326	2.44	*n*				*n*	
GaAs + $[Co^{III}(NH_3)_6]^{3+}$	15	19.0	*p*	41.0	991		43.6	282	1.6×10^{-9}	*p*			780.5	12481	1.7×10^{-8}	530.8	47682	1.87	*n*				*o*	
0.010 M KOH	35	19.0	*p*	40.9	889		43.5	261	1.4×10^{-9}	*p*			780.5	12098	1.4×10^{-8}	530.8	47354	1.92	*n*				*o*	
RT	50	18.6	*p*	40.6	808		43.5	330	1.5×10^{-9}	*p*			480.8	14404	1.2×10^{-8}	530.9	56474	1.92	*n*				*o*	
	65	18.5	*p*	40.4	391		43.5	220	1.3×10^{-9}	*p*			781.9	12295	9.3×10^{-9}	532.0	58688	2.34	*n*				*o*	
GaAs + $[Co^{III}(NH_3)_6]^{3+}$	30	19.4	3164	41.4	2937	0.93	44.0	104	2×10^{-10}	20.7	91	3×10^{-10}	(781)[q]	<100[r]	<2 × 10^{-10}	533.3	9939	*m*	*n*				2000	2.3×10^{-9}
pH = 12.9 (satd NH_3)																							
$T \approx 180$ K																							
GaAs + $[Co^{III}(NH_3)_5(OH)]^{2+}$	30	19.5	3114	41.5	2517	0.81	44.7	328	7×10^{-10}	21.3	110	3×10^{-10}	780.8	8114	8.2×10^{-9}	532.4	50950	2.16	*n*				4452	2.6×10^{-9}
0.010 M KOH, RT																							
GaAs + $[Co^{III}(NH_3)_5(OH_2)]^{3+}$	30	19.5	14664	41.5	13659	0.93	43.6	188	<2 × 10^{-10}	21.2	226	<2 × 10^{-10}	*m*			532.0	12070		*n*				1748	6×10^{-10}
0.10 M HCl, RT																							
GaAs + $[Co^{III}(NH_3)_5N_3]^{2+}$	65	19.3	2628	41.2	1815	0.69	43.5	306	5×10^{-10}	21.0	98	1×10^{-10}	*m*			531.9	13790		*n*				8137	3.5×10^{-9}
pH = 6.2 (MES buffer)[s]																							
$T \approx 180$ K																							
GaAs + $[Co^{III}(NH_3)_5Br]^{2+}$	30	19.4	*p*	41.4	272		44.5	99	1.9×10^{-9}	*p*			782.1	18218	2.4×10^{-8}	532.1	18247	2.04	*n*				887	2×10^{-10}
0.010 M KOH, RT																							
GaAs + $[Co^{III}(NH_3)_5Br]^{2+}$	30	19.7	11673	41.7	10869	0.93	43.5	150	<2 × 10^{-10}	21.3	119	<2 × 10^{-10}	*m*			532.5	13060	*m*	*n*				7574	2.4×10^{-9}
0.10 M HCl, RT																							
GaAs + $[Co^{III}(bpy)_3]^{3+}$	30	19.1	2361	41.2	2980	1.26	43.7	315	6×10^{-10}	21.0	*o*		*m*			531.8	19817		*n*				12389	7.4×10^{-9}
pH = 11.3, RT[s]	50	19.0	1905	41.2	2495	1.31	43.7	295	5×10^{-10}	21.0	*o*		*m*			531.8	20060		*n*				12500	6.0×10^{-9}
	60	19.1	1491	41.3	1810	1.21	43.9	300	5×10^{-10}	21.1	*o*		*m*			531.8	19858		*n*				11440	5.1×10^{-9}
	65	19.0	1148	41.3	1654	1.44	44.0	288	5×10^{-10}	21.1	*o*		*m*			531.8	21416		*n*				*o*	
GaAs + $[Co^{III}(bpy)_3]^{3+}$	30	19.5	10108	41.5	10649	1.05	43.5	73	<2 × 10^{-10}	*m*			*m*			532.4	13670		*n*				8009	2.7×10^{-9}
0.10 M HCl, RT[s]																							
GaAs + $Co^{II}(aq)^{2+}$	30	19.2	7684	41.2	6790	0.88	43.3	191	<2 × 10^{-10}	*m*			781.3	6383	3.9×10^{-9}	531.5	34565	2.02	*n*				2591	1.2×10^{-9}
0.010 M KOH, RT																							
GaAs + $Co^{II}(aq)^{2+}$	30	19.4	3164	41.4	2937	0.93	44.0	104	≤2 × 10^{-10}	20.7	91	2×10^{-10}	(782)[q]	<300[r]	<6 × 10^{-10}	533.3	9939		*n*				2000	2.3×10^{-9}
pH = 12.9 (satd NH_3)																							
$T \approx 180$ K																							
GaAs + $Co^{II}(aq)^{2+}$	30	19.3	11451	41.3	10271	0.90	43.1	215	<2 × 10^{-10}	*m*			*m*			532.2	14050		*n*				8556	2.8×10^{-9}
0.10 M HCl, RT																							
GaAs + $[Co^{II}(bpy)_3]^{2+}$	65	19.1	3901	41.3	7315	1.88	*m*			*m*			(781)[q]	<200[r]	<2 × 10^{-10}	531.8	16377		*n*				9438	1.9×10^{-9}
pH = 12.0, RT[s]																							
GaAs + $[Co^{II}(bpy)_3]^{2+}$	30	19.4	11330	41.4	10723	0.95	42.9	224	<2 × 10^{-10}	*m*			*m*			532.3	9119		*n*				7748	2.5×10^{-9}
0.10 M HCl, RT[s]																							
GaAs + $[Co^{III}(NH_3)_6]^{3+}$	0	19.1	1436	41.2	1071	0.75	44.1	197	1.2×10^{-9}	20.3	124	1.0×10^{-9}	59.0[t]	376[u]		531.2	7427		54.4	675	1.6×10^{-9}	1.79	*o*	
(0.010 M KOH)	70	19.2	724	41.2	595	0.82	43.7	198	7×10^{-10}	20.5	50	7×10^{-10}	59.0[t]	381[u]		531.1	*o*		54.0	687	1.5×10^{-9}	1.80	*o*	
+ KOH-$Se^{-/2-}$ $T \approx 180$ K																							

[a] Coverage is presented as total moles projected onto 1 cm^2 ≡ mol cm^{-2}. [b] Angle between surface normal and photoelectron detector axis. [c] All peak positions are reported in binding electron volts (BeV) and are referenced against C 1s = 284.6 BeV. [d] Intensities (counts per second per eV) normalized with respect to photoelectron cross-section, escape depth, and atomic number density, except for O 1s, which is given as the raw intensity (counts per eV) normalized by the scan duration. [e] Ratio of normalized peak intensities. [f] Coverage calculated assuming the density of vitreous As_2O_3. [g] Coverage calculated based on the average of the densities for α and β Ga_2O_3. [h] Coverage calculated based on the density of *roseo*-$Co(OH)_2$. [i] Corrected O 1s intensity derived from total O 1s signal by subtraction of counts due to substrate oxides and H_2O, and then normalized as in note *d*. [j] Coverage assuming the density of trogtalyte, $CoSe_2$; cobalt intensity based on Co 3p lines. [k] Coverage calculated assuming an average hydrocarbon density. See experimental for details. [l] Approximate (±10 K) temperature of sample during analysis. [m] No peak observed above background. [n] Region not analyzed. [o] Peak position determined, area not deconvoluted. [p] Peak position obscurred by O 2s line. [q] Edge of poorly defined peak barely discernible above background. [r] Estimate of upper limit of intensity. [s] No N 1s signal above background; no signal above background due to counterions. [t] Co 3p peak position. [u] Normalized Co 3p peak intensity.

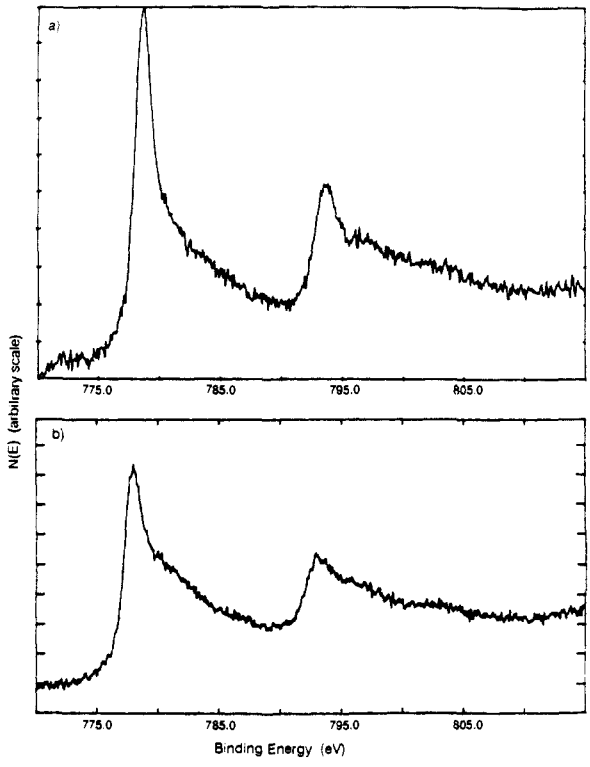

Figure 5. Co 2p region XPS; the raw data are displayed corrected for binding energy relative to C 1s (a) etched (100)-oriented n-GaAs substrate exposed to basic (pH = 12) 0.010 M $[Co^{III}(NH_3)_6]^{3+}$ complex and subsequently immersed in 1.0 M KOH–0.8 M K_2Se–0.2 M K_2Se_2 electrolyte; (b) Ar^+ ion sputtered sample of CoSe set in In foil.

GaAs surface. For 0.010 M KOH solutions, we observed weaker (relative to substrate GaAs signals) Co 2p and O 1s signal intensities from $[Co^{II}(H_2O)_6]^{2+}$-treated GaAs samples than from Co(III) ammine treated GaAs (Tables I and II). XPS performed on (100) n-GaAs substrates exposed to 0.010 M KOH solutions of $[Co^{II}(OH_2)_6]^{2+}$ showed no evidence of substrate oxidation above background levels ($\leq 2 \times 10^{-10}$ mol·cm^{-2}). Consistently, total coverages of cobalt were in the low end of the range obtained from exposure of GaAs to Co(III) ammine complexes.

As was found for the Co(III) ammine complexes, GaAs surfaces exposed to $[Co^{II}(H_2O)_6]^{2+}$ solutions of 0.10 M HCl displayed no detectable Co XPS signals. Furthermore, GaAs surfaces laden with a $Co(OH)_2$ precipitate and then exposed to ammonia solutions (14.8 M NH_3, pH = 12.9) showed no signals due to Co(II) remaining in the XP spectra. Consistently, GaAs samples that had been exposed to Co(II) solutions in concentrated aqueous ammonia also yielded no resolvable Co 2p XPS signals above background. NH_3 stabilizes Co(II) as $[Co^{II}(NH_3)_6]^{2+}$ relative to $Co(OH)_2$;[36] thus, this complexation reaction effectively competes with the deposition of $Co(OH)_2$ onto GaAs surfaces.

2. XPS Studies of Co Chemisorption on GaAs: Properties after Exposure to Aqueous KOH–K_2Se–K_2Se_2 Solutions. XPS data were also obtained for GaAs samples that had been exposed to aqueous solutions of 1.0 M KOH–0.8 M K_2Se–0.1 M K_2Se_2 after chemisorption of Co.[8] Both (100)-oriented n-type single crystals and powdered GaAs samples displayed Co 2p XPS peaks at 778.4 and 793.3 BeV (Figure 5a). In contrast to Figure 1, these spectra showed no satellite structure. A wide (0–1100 BeV) XP scan showed only the presence of signals from As, Ga, C, Se, O, and Co (Table I). Identical Co 2p spectra were obtained from GaAs that had been exposed to $[Co^{III}(NH_3)_5X]^{n+}$ (X = NH_3, OH^-, Br^-) (0.010 M KOH) or to $[Co^{II}(OH_2)_6]^{2+}$ complexes (0.010 M KOH) and then immersed in the KOH-$Se^{-/2-}$ solution. We observed from low (ca. $^1/_2$ monolayer) to no detectable ($<^1/_4$ monolayer by XPS) Se 3d peak intensity on etched GaAs samples exposed only to $Se^{-/2-}$ electrolyte. Large-intensity (>2 monolayer) persistent Se 3d signals were observed only on GaAs substrates that also possessed surface-bound Co(II).

A comparison of Figures 1 and 5a clearly shows that the adsorbed Co has undergone a chemical reaction with the KOH-$Se^{-/2-}$ electrolyte. In contrast to the $[Co^{III}(NH_3)_6]^{3+}$ or $Co(OH)_2$ spectra of Figure 2, the Co 2p features in Figure 5a are comparable to those reported previously for the low-spin cobalt chalcogenides[39] and to spectra obtained in our work from a sputtered sample of authentic CoSe (Figure 5b). The presence of Se in the overlayer, the lack of any observable Co 2p satellite structure, and the absence of counterions such as K^+ strongly suggest that Se^{2-} has reacted with the Co(II) sites and has been introduced into the inner sphere of surface-bound Co.

The stoichiometry of the resulting surface phase was estimated to be $Co_{1.0}Se_{1.8}$. We observed, however, a raw intensity ratio Co(2p)/O(1s) $\approx$ 3 in the surface-bound film and therefore must consider the possibility of a mixed seleno–oxo inner sphere for cobalt. An argument against this scenario comes from the fact that oxo and hydroxo are relatively weak field ligands and would be expected to lead to high-spin Co(II), and hence satellite lines in the Co 2p XPS. Assuming an atomic density of 4.7×10^{-2} mol·cm^{-3} (which is the average of the atomic densities for $Co(OH)_2$ and $CoSe_2$), the Co/O/Se intensity ratio (normalized to Co) would, at the upper limit of complete oxygen incorporation into the inner sphere of Co(II), represent a composition $Co_{1.0}Se_{0.7}O_{1.3}$. These stoichiometry data are useful in assessing the EXAFS data in section 3.B for the identity of the Co inner-shell scatterers.

Analysis of the angle-resolved XPS data showed that after exposure to the KOH-$Se^{-/2-}$ electrolyte, the Co(II)-containing surface layer was inhomogeneous. Additionally, the Co–Se coverages were not substantially reduced compared to the amount of Co adsorbed from the aqueous Co(III) or Co(II) solutions. Table II summarizes the Co and Se coverage data. In general, $Se^{-/2-}$ exposure of surface-bound Co ion always resulted in the transformation of the Co 2p peaks from a high-spin Co(II) state to a low-spin Co(II) state, as well as resulting in the appearance of Se signals in the XPS.

3. X-ray Absorption and Fluorescence Spectra: Properties in Vacuo and in Aqueous Solution. A. GaAs Exposed to Aqueous Co(III) Complexes. In order to obtain further information on the coordination environment of the GaAs-bound Co, X-ray absorption and fluorescence studies were performed. Amplitude and phase parameters for specific absorber–scatterer pairs were obtained from EXAFS data for the model compounds $Co(OH)_2$, $CoSe_2$, $[Co^{II}(OH_2)_6](ClO_4)_2$, CoO(OH), and $CoAs_3$. Potential first-shell and second-shell absorber–scatterer interactions were isolated by application of Fourier filtering techniques on k^3 weighted data.[30c-f]

Figure 6 displays the Co K edge spectra, Co-based EXAFS (taken in the fluorescence mode), and Fourier transform of the EXAFS for GaAs powder treated with $[Co^{III}(NH_3)_5(OH)]^{2+}$. For comparison, Figure 7 displays the X-ray absorption spectra and Fourier transformed EXAFS for two model compounds, $Co^{II}(OH)_2$ and $Co^{III}O(OH)$.

The position of the Co K edge in Figure 6a verifies that the GaAs-bound Co is in the Co(II) oxidation state. Edge position data taken at 77 K for $[Co^{II}(OH_2)_6](ClO_4)_2$, CoO(OH) (Table III), and other Co(II) and Co(III) model complexes are consistent with this assignment. This assignment is also consistent with the oxidation state deduced from the Co 2p binding energy, peak splittings, and satellite structure observed in the XP spectra (vide supra).

A summary of the EXAFS data analysis is presented in Table III. For the Co/GaAs sample, the first shell around Co was found to consist of (6 ± 1) second-row atoms (most likely N or O) at (2.08 ± 0.05) Å, and the second shell consisted of (7 ± 1) third-row scatterers at (3.13 ± 0.05) Å. The XPS analysis of these samples strongly indicated that the light element was O, because no N (above background) was found to support the required Co:N mass balance (Table I). The 2.08 Å first shell bond distance is in excellent accord with that found by EXAFS and X-ray dif-

(39) Mandle, A. B.; Badrinarayanan, S.; Date, S. K.; Sinha, A. P. B. *J. Electron Spectrosc. Relat. Phenom.* **1984**, *33*, 61.

Table III. EXAFS Derived Nearest Neighbor Distances and Coordination Numbers

experiment[a]	1st shell d_{Co-O} (Å)	1st shell N_O	2nd shell d_{Co-Co} (Å)	2nd shell N_{Co}	absorption edge (eV)[b]
roseo-$Co(OH)_2$[c], T = 77 K[d]	2.097	6.0	3.17	6.0	7719.7
$[Co^{II}(OH_2)_6](ClO_4)_2$[e], T = 77 K	2.085	6.0			7720.1
$CoO(OH)$[f], T = 77 K	1.90[g]	6.0			7721.3
	2.69[h]	4.0			
GaAs + $[Co^{III}(NH_3)_5(OH)]^{2+}$ 0.010 M KOH, T = 10 K	2.08 ± 0.05	7 ± 1[i]	3.13 ± 0.05	7 ± 1[i]	7720.7
T = 77 K	2.08 ± 0.05	8 ± 1[i]	3.13 ± 0.05	8 ± 1[i]	7720.3
T = 298 K	2.08 ± 0.05	7 ± 1[i]	3.14 ± 0.05	7 ± 1[i]	7720.8
GaAs + $[Co^{III}(NH_3)_5(OH)]^{2+}$ 0.010 M KOH slurry, T = 298 K	2.09 ± 0.05	6 ± 1	3.13 ± 0.05	7 ± 1[i]	7720.7
GaAs + $Co^{II}(aq)^{2+}$ 0.010 M KOH, T = 10 K	2.08 ± 0.05	6 ± 1	3.13 ± 0.05	8 ± 1	7720.3

experiment	1st shell d_{Co-Se} (Å)	1st shell N_{Se}	2nd shell d_{Co-Co} (Å)	2nd shell N_{Co}	absorption edge (eV)[b]
$CoSe_2$[j]	2.42	6.0			7716.2
GaAs + $[Co^{III}(NH_3)_6]^{3+}$(0.010 *M* KOH) + KOH-$Se^{-/2-}$, T = 77 K	2.36 ± 0.05	5.3 ± 1			7717.1
GaAs + $[Co^{III}(NH_3)_5(OH)]^{2+}$ (0.010 *M* KOH) + KOH-$Se^{-/2-}$, T = 10 K	2.34 ± 0.05	4.6 ± 1			7719.0

[a] Range of k and R-space values used in all fits: $k(Å^{-1})$ = {3.2–12.75}, R(Å) = {0.00–7.50}; R interval = 0.025. Scattering distances and coordination numbers for model compounds were obtained from X-ray diffraction studies and are shown here for reference. [b] Taken as the energy of the half-height of the absorption edge. [c] From ref 40. [d] T at which EXAFS data collected. [e] From ref 31. [f] From ref 15b. [g] d_{Co-O} distance. [h] d_{Co-OH} distance. [i] Coordination numbers higher than expected due to Cu fluorescence interference from the sample mount. [j] From ref 16b,c.

fraction for the first shell Co–O distance in *roseo*-$Co(OH)_2$ (d_{Co-O} = 2.097 Å).[40] It also is longer than typically observed for Co(III)–O distances in compounds with all octahedral sites occupied by oxygen, such as tris(acetylacetonato)cobalt(III) (average d_{Co-O} = 1.888 Å),[41] which further confirms the oxidation state assignment as Co(II).

The relatively high coverage (up to 2.4 × 10^{-8} mol·cm^{-2}) of Co from the XPS and radioisotope data (vide infra) supports the assignment of the predominant second-shell scatterer to Co. The second-shell distance for the GaAs-bound Co is within 0.017 Å of the Co–Co distance in $Co(OH)_2$,[40] and this is consistent with the existence of a network solid that would be expected from the redox deposition mechanism of Co onto GaAs.[42] Angle-resolved XPS analysis (vide supra) of these samples yielded an upper limit on the As_2O_3/Co mol ratio of 0.16 and an upper limit on the Ga_2O_3/Co mol ratio of 0.05. These observations strongly suggest that most of the second-shell EXAFS scattering is due to Co–Co backscattering. Thus, the combined EXAFS and XPS data yield a structure for the adsorbed Co that is closely analogous to that of bulk $Co(OH)_2$. At present, the relatively high Co coverages, combined with the similar scattering properties of the third-row elements Co, Ga, and As, have precluded direct observation of the Co–Ga or Co–As surface bonding in this system. However, by comparison of fits to the data displayed in Figure 6 with model EXAFS data obtained from $CoAs_3$, we can confidently rule out direct Co–As first-shell coordination as the predominant mode of Co chemisorption onto GaAs powders.

Figure 8 displays the Fourier transformed EXAFS data for a $[Co^{III}(NH_3)_5(OH)]^{2+}$-treated GaAs sample that had been evacuated and held sequentially at 10, 77, and 298 K. The data from the aqueous slurry of GaAs powder at 298 K, also depicted in Figure 8, were very similar to that for the cooled and evacuated samples, except for the minor differences expected from a reduction in Debye–Waller factors at the lower temperatures. We thus take the analysis of the low-temperature data sets, summarized in Table III, to be good representations of the coordination structure for the adsorbed Co while in contact with the aqueous electrolyte.

Exposure of GaAs powder to a basic solution of $[Co^{II}(OH_2)_6]^{2+}$ ions gave Co K edge and EXAFS data (Figure 9) that were extremely similar to that obtained from $Co(OH)_2$ (Figure 7). The results of the EXAFS fits to this data are also summarized in Table III.

B. GaAs Exposed to Aqueous Co(III) Complexes and KOH–$Se^{-/2-}$ Electrolyte. Figure 10 shows the Co EXAFS and Fourier transformed EXAFS amplitude of GaAs powders that had been exposed to $[Co^{III}(NH_3)_5(OH)]^{2+}$ or $[Co^{III}(NH_3)_6]^{3+}$ ions and then exposed to 1.0 M KOH–0.8 M K_2Se–0.1 M K_2Se_2 solutions. The scattering amplitude and phase factor for the Co–Se absorber–scatterer pair were obtained from an EXAFS experiment performed on pure single-phase $CoSe_2$ (synthetic Trogtalyte). The best fits to the EXAFS data are presented in Table III.

A comparison of Figure 10 to Figure 6 shows that the Co coordination sphere was substantially altered as a result of exposure to the KOH-$Se^{-/2}$ electrolyte. These results are consistent with changes in the XP spectra between the two samples (Figures 1 and 5). Fits to the EXAFS indicated a Co inner-shell composition of 5 ± 1 Se. This EXAFS fit represents a composition close to $CoSe_2$, which is in reasonable agreement with the composition deduced from XPS data.

Attempts to fit the EXAFS data with parameters for both selenium and oxygen in cobalt's inner shell led to unphysical results. While reasonable first-shell scattering distances (d_{Co-X}) could be obtained, these two-component fits were always accompanied by unrealistic values for the number (>10) of nearest-neighbor scatterers about Co. Similarly, fits attempted using only oxygen shell parameters never gave good values for the nearest-neighbor distances or for the number of scatterers. Only the use of selenium scattering parameters led to good fits to the EXAFS data. Taken together with evidence from XP spectra on identically treated surfaces, the EXAFS data support the hypothesis that most of the oxygen is no longer bound to Co(II) following reaction in basic selenide electrolyte.

4. Quantitative Analyses of Co Chemisorption on GaAs: pH Dependence and ^{57}Co Radiotracer Experiments. Wet Chemical Studies. An interesting feature of the GaAs/Co(III) chemisorption process is the lack of detectable Co in either the XP or X-ray absorption spectra for GaAs exposed to Co(III) in acidic media. To ascertain the pH dependence and overall stoichiometry of the Co(III)–GaAs chemisorption reaction, GaAs powder was treated

(40) Lotmar, W.; Feitknecht, W. *Z. Kristallogr.* **1936**, *93*, 368.
(41) Kruger, G. J.; Reynhardt, E. C. *Acta Crystallogr. Sect. B: Struct. Sci.* **1974**, *B30*, 822.
(42) (a) Dillard, J. G.; Schenk, C. V. In *Geochemical Processes at Mineral Surfaces*; Davis, J. A., Hayes, K. F., Eds.; ACS Symposium Series 323; American Chemical Society: Washington, D.C., 1986; pp 503–522. (b) Parks, G. A. *Chem. Rev.* **1965**, *65*, 177. (c) Benjamin, M. M.; Leckie, J. O. *J. Colloid Interface Sci.* **1981**, *79*, 209. (d) Benjamin, M. M.; Leckie, J. O. *J. Colloid Interf. Sci.* **1981**, *83*, 410. (e) Benjamin, M. M.; Leckie, J. O. *Environ. Sci. Technol.* **1982**, *16*, 162.

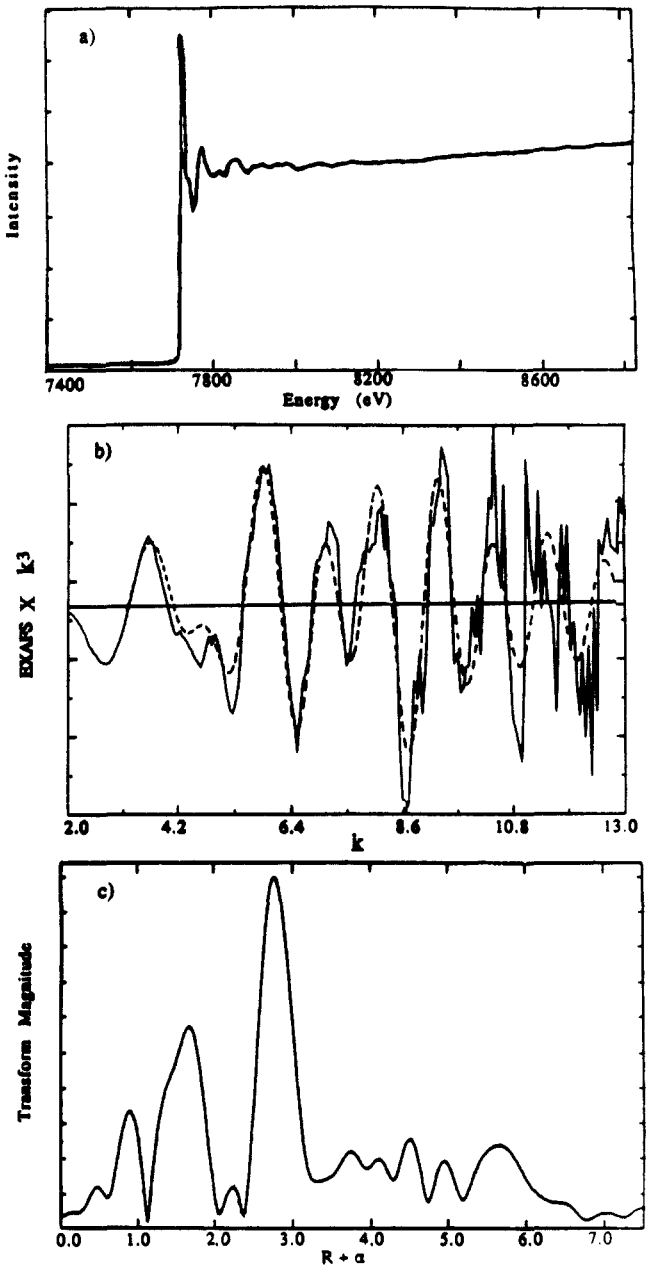

Figure 6. Co K-edge X-ray fluorescence spectrum. Data for GaAs powder treated with a pH = 12 (KOH) solution of 0.010 M $[Co^{III}(NH_3)_5(OH)]^{2+}$, collected at room temperature on an unfocussed beam line at 10^{-6} Torr; (a) Raw X-ray fluorescence data. (b) k^3 weighted EXAFS extracted from spectrum a. Superimposed on the raw data is the fit (dashed curve) obtained from the summation of individual fits to the first-shell (Co–O) and second-shell (Co–Co) scattering contributions. (c) Fourier transform of the EXAFS in b.

with aqueous solutions containing $[Co^{III}(NH_3)_6]^{3+}$ or $[Co^{III}(bpy)_3]^{3+}$, and the resulting solution was subjected to analysis by wet chemical and X-ray fluorescence methods, or to UV–vis spectrophotometry.

In HEPES buffer (pH = 7.4) or 14.8 M NH_4OH (pH = 12.9), we observed the quantitative reduction of $[Co^{III}(NH_3)_6]^{3+}$ to Co(II) by GaAs powder (Table IV). The resulting solutions also contained increased concentrations of soluble As and Ga species, which were analyzed by XRF methods. This yielded relative ratios of [As]:[Ga]:[Co], normalized to the As concentration, of 1.0 ± 0.2:1.0 ± 0.2:6.0 ± 0.6. These data clearly indicate a six-electron-transfer process in the oxidation of 1 equiv of GaAs. Additional evidence for electron transfer between GaAs and Co(III) complexes at high pH was obtained by UV–vis spectrophotometric methods. Solutions (pH = 11.7) of $[Co^{III}(bpy)_3]^{3+}$ in contact with GaAs powder were observed to undergo quantitative reduction to $[Co^{II}(bpy)_3]^{2+}$. These processes are consistent with the Co(II) oxidation state obtained from the XPS and X-ray absorption data analysis of GaAs samples exposed to basic 0.010 M $[Co^{III}(NH_3)_5X]^{n+}$ (X = NH_3, N_3^-, OH^-, Br^-) solutions.

In 0.10 M HCl, only low levels (<300 μM) of Co(II) were found spectrophotometrically in the reaction solution, and only small amounts of $[Co^{III}(NH_3)_6]^{3+}$ were observed (by UV–vis spectroscopy) to react with GaAs. The concentrations of soluble As and Ga species detected by XRF were also low and were near that of the background levels found when GaAs powder was treated with 0.10 M HCl. Furthermore, pH = 1.7 solutions of $[Co^{III}(bpy)_3]^{3+}$ in contact with GaAs powder were not observed spectrophotometrically to produce $[Co^{II}(bpy)_3]^{2+}$, or to deplete the absorbance of $[Co^{III}(bpy)_3]^{3+}$ due to adsorption of Co onto the GaAs. In 0.10 M HCl, both Co(II) aquo ions and oxides of the GaAs are soluble, making it unlikely that the reaction would be impeded by an insoluble oxide layer on the GaAs. We therefore conclude that the Co(III) species investigated are not reactive with GaAs in 0.10 M HCl on our experimental time scale.

To assess the reactivity of GaAs in 0.10 M HCl with suitable oxidants, GaAs powders were exposed to $[Fe^{III}(H_2O)_6]^{3+}$. X-ray fluorescence analysis of GaAs solutions exposed to Fe^{3+} in 0.10 M HCl showed that six electrons per GaAs equivalent were consumed in the reaction (Table IV). This result demonstrates that, given a sufficiently powerful oxidant, GaAs will react by a net six-electron redox pathway in 0.10 M HCl.[37] This strongly suggests that the lack of reactivity of GaAs with $[Co^{III}(NH_3)_5X]^{n+}$ (X = Br^-, OH_2) (0.10 M HCl) and $[Co^{III}(bpy)_3]^{3+}$ (pH = 1.7) arises from thermodynamic considerations as opposed to oxide dissolution limitations.

The pH stability of $Co(OH)_2$ bound to GaAs was assessed by exposing GaAs powder that had been previously reacted with $[Co^{III}(NH_3)_6]^{3+}$ in 0.010 M KOH to solutions of 0.10 M HCl, phosphate buffer (pH = 7.0), or 0.010 M KOH and analyzing the resulting solution for Co(II) spectrophotometrically.[32] In 0.010 M KOH, no Co(II) was detected in the rinse solution. However, in 0.10 M HCl, or phosphate buffer (pH = 7.0), all of the Co(III) that reacted with the GaAs was liberated as Co(II) and was detected as the soluble Co(II) thiocyanate complex. These results verify that if GaAs had reacted with Co(III) at 0.10 M HCl, the reaction products would have been detected in the solution phase. They also confirm that XPS analysis of the GaAs surface composition in 0.010 M KOH should yield an accurate measure of the amount of $Co(OH)_2$ formed due to the reactions of interest.

5. ^{57}Co(III) Ammine Studies of Co Chemisorption on GaAs. As a check on the Co coverages obtained from the XPS data analysis, (100) n-GaAs single crystals were treated with 34.0 μCi/mL enriched $[^{57}Co^{III}(NH_3)_6]^{3+}$ in 3.46 mM total $[Co^{III}(NH_3)_6]^{3+}$ solution in base (pH = 12.0, KOH(aq)). The samples were then removed from the γ-active Co solution, and the GaAs surface was etched to remove approximately 0.5 μm of GaAs. The Co in the etch effluent and the remaining GaAs were then analyzed for γ-activity. No radioactivity above background was observed for treated and etched GaAs samples, while the effluent displayed γ-ray counts consistent with 5–8 $Co(OH)_2$-equivalent monolayers (1 monolayer $Co(OH)_2$ = 1.4×10^{-9} mol·cm^{-2}) adsorbed onto (100) GaAs.

The pH dependence of the Co chemisorption was also investigated by these radiotracer methods. GaAs crystals exposed to $[^{57}Co^{III}(NH_3)_6]^{3+}$ solutions at pH = 1.0 yielded no γ-ray counts above background (Table V). Additionally, GaAs substrates that were initially exposed to pH = 12.0 $[^{57}Co^{III}(NH_3)_6]^{3+}$ solutions and then immersed in pH = 1.0 HCl for 30 s passed all ^{57}Co to the acidic rinse solution. The subsequent γ-activity of the acid rinse solutions represented 5–6 $Co(OH)_2$-equivalent monolayers. These experiments offer estimates of Co chemisorption onto GaAs surfaces consistent with, and independent of, XPS measurements. They also confirm the XRF analyses regarding the pH stability of surface-bound $Co(OH)_2$ on GaAs.

Discussion

The above data allow us to distinguish between three possible pathways for the chemisorption of Co(III) onto GaAs: electro-

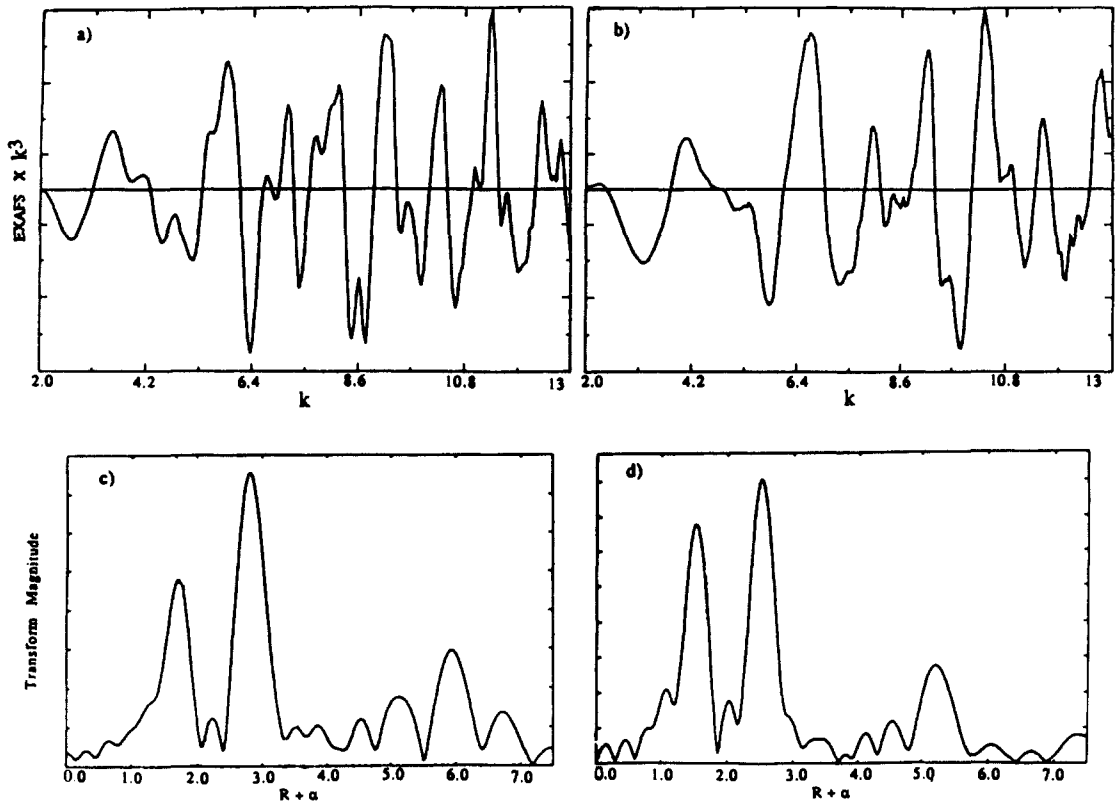

Figure 7. k^3 weighted EXAFS and Fourier transform data for model compounds *roseo*-$Co^{II}(OH)_2$ and $Co^{III}O(OH)$. Spectra were collected in transmission mode at 77 K on a focussed beam line at 10^{-6} Torr: (a) Co K-edge EXAFS of *roseo*-$Co(OH)_2$. (b) Co K-edge EXAFS of CoO(OH). (c) Fourier transform of a. (d) Fourier transform of b.

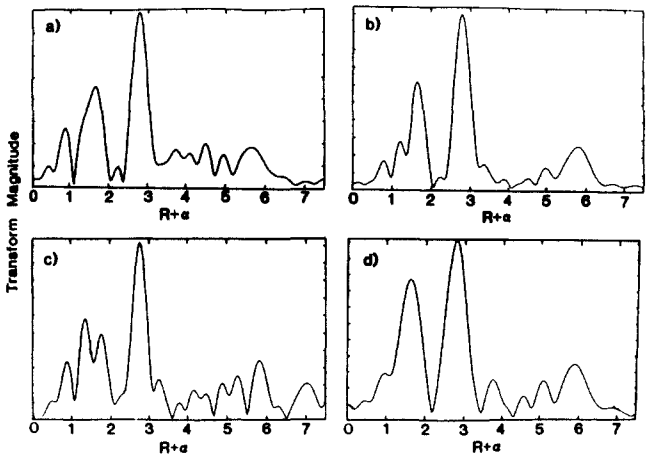

Figure 8. In vacuo and in situ comparison of Fourier transformed Co K-edge EXAFS of GaAs powder treated with a pH = 12 (KOH) solution of 0.010 M $[Co^{III}(NH_3)_5(OH)]^{2+}$. Data collected in fluorescence mode. Each panel displays a different temperature and contacting environment for the Co complex treated powder. (a) T = ambient, $p = 10^{-6}$ Torr. (b) $T = 77$ K, $p = 10^{-6}$ Torr. (c) $T = 10$ K, $p = 10^{-6}$ Torr. (d) Powder in contact with pH = 12 (KOH) aqueous solution at ambient temperature and pressure (N_2).

static binding of the complex to charged sites on the semiconductor surface,[43] substitution of a ligand site on Co(III) by a surface-attached ligand group, and a redox reaction to produce a labile Co(II) oxidation state. The absence of detectable chemisorption for $[Co^{III}(bpy)_3]^{3+}$ or $[Co^{II}(bpy)_3]^{2+}$ over a range of pH values implies that electrostatic forces alone are not sufficient to explain the observed reactions with the $[Co^{III}(NH_3)_5X]^{n+}$ (X = NH_3, OH_2, Br^-, N_3^-, OH^-) complexes. Ligand substitution on $[Co^{III}(NH_3)_5X]^{n+}$ (X = NH_3, OH_2, Br^-, N_3^-, OH^-) complexes is far too slow to account for the observed Co chemisorption: at pH = 1.0 and 0.01 M $[Co^{III}(NH_3)_5X]^{n+}$ (X = Br^-, OH_2), the half-life of surface ligands should be from 10^7 to 10^{11} s, while at pH = 10 it should be ca. 10^{10} s.[36] In contrast, ^{57}Co(III) ammine experiments reveal that ca. 1.1×10^{-8} mol·cm^{-2} of Co can be adsorbed on GaAs in ≤60 s. Furthermore, anation on a Co(III) site should result in XPS signals attributable to the remaining NH_3 groups and should also result in Co 2p XPS signals and X-ray absorption edge features that are characteristic of $[Co^{III}(NH_3)_5X]^{n+}$ (X = NH_3, OH_2, Br^-, N_3^-, OH^-) complexes. The absence of such signals in the XPS and EXAFS data demonstrates that a Co(III) substitutional pathway cannot be a dominant process in the chemisorption of Co onto GaAs. Additionally, the observation of identical surface chemical behavior from experiments performed on GaAs surfaces in the dark indicates that the reaction is thermal in nature and is not initiated by photochemical events on either the substrate or the metal complex. Our data therefore strongly suggest that a redox process to yield Co(II) is the dominant binding pathway.

Quantitative chemical analysis of solutions of GaAs and Co(III) ammines provides excellent evidence for a redox-dominated chemisorption pathway. In 14.8 M NH_4OH (pH = 12.9), complete reduction of $[Co^{III}(NH_3)_6]^{3+}$ by GaAs was observed spectroscopically, and a stoichiometric amount of Co(II) was produced. To within experimental error, the relative concentrations of [As]:[Ga]:[Co] as determined by X-ray fluorescence studies are consistent with the consumption of six electrons in the oxidation of 1 equiv of GaAs by Co(III):

$$6[Co^{III}(NH_3)_6]^{3+} + GaAs \rightarrow 6Co^{II} + Ga^{3+} + As^{3+} + 36NH_3 \quad (1)$$

This reaction has precedence in the electrochemical dissolution studies of GaAs reported by Gerischer and Memming[37] and is consistent with the previous estimate of the redox potential of GaAs obtained from Born-Haber cycles and rotating disk corrosion

(43) (a) Tschapek, M.; Wasowski, C.; Torres Sanchez, R. M. *J. Electroanal. Chem.* **1976**, *74*, 167. (b) Uchida, I.; Akahoshi, H.; Toshima, S. *J. Electroanal. Chem.* **1978**, *88*, 79.

Table IV. Distribution of Product Ions by XRF Analysis

experiment	raw counts[a] As	Ga	M[c]	Br[d]	concentration, mM[b] [As]	[Ga]	[M][c]
GaAs + $[Co^{III}(NH_3)_6]^{3+}$	4836.4	2728.9	2120.4	1304.4	1.11	1.05	6.19
satd NH_3, pH = 12.9	3980.5	2461.4	2170.6	1358.9	0.88	0.91	6.08
	4561.4	2752.8	1978.0	1137.3	1.20	1.22	6.62
			average of concentrations:		1.1 ± 0.2	1.1 ± 0.2	6.3 ± 0.3[e]
	ratio of average concentrations, relative to [As]:				1.0 ± 0.2	1.0 ± 0.2	5.9 ± 0.3
GaAs + $[Co^{III}(NH_3)_6]^{3+}$ CAPS buffer, pH = 10.6	*f*	*f*	*f*				
GaAs + $[Co^{III}(NH_3)_6]^{3+}$ HEPES buffer, pH = 7.4	889.2	605.8	547.5	765.5	0.20	0.19	1.19
	ratio of concentrations, relative to [As]:				1.00	0.93	5.98
GaAs + $[Co^{III}(NH_3)_6]^{3+}$ 0.1 M HCl, pH = 1.0	*g*	*g*	*g*				
GaAs + $Fe^{III}Cl_3$(aq) 0.1 M HCl, pH = 1.0	577.5	376.8	455.1	3287.7	0.30	0.27	1.82
	ratio of concentrations, relative to [As]:				1.00	0.90	6.06

[a] Acquisition times: at pH = 12.9, 500 s; all others 300 s. [b] Raw counts converted to concentrations by the use of empirically determined cross-sections, σ, relative to $\sigma_{Br} \equiv 1$, and the equation $[X] = CTS_x \cdot \sigma \cdot [Br]/CTS_{Br}$. Cross-sections were found to be solution composition dependent. At pH = 12.9: $\sigma_{Co} = 12.82$; $\sigma_{AS} = 1.011$; $\sigma_{Ga} = 1.694$. At pH = 7.4: $\sigma_{Co} = 16.47$; $\sigma_{As} = 1.698$; $\sigma_{Ga} = 2.308$. At pH = 1.0: $\sigma_{Fe} = 14.05$; $\sigma_{As} = 1.698$; $\sigma_{Ga} = 2.308$. [c] M = Co or Fe, see experiment column. [d] Counts from KBr internal standard. At pH = 12.9, [Br] = 0.297 mM. At pH = 7.4, [Br] = 0.101 mM. At pH = 1, [Br] = 1.01 mM. [e] Increase in [Co] over initial value of 5.00 mM is due to a decrease in the solution volume from loss of NH_3(g). An independent check by UV-vis at the end of the reaction period gave $[Co^{II}]$ = 5.80 mM. Further losses in air account for the final state concentration. [f] Not possible to measure at this pH. See text for discussion. [g] No detectable reaction for this system at this pH.

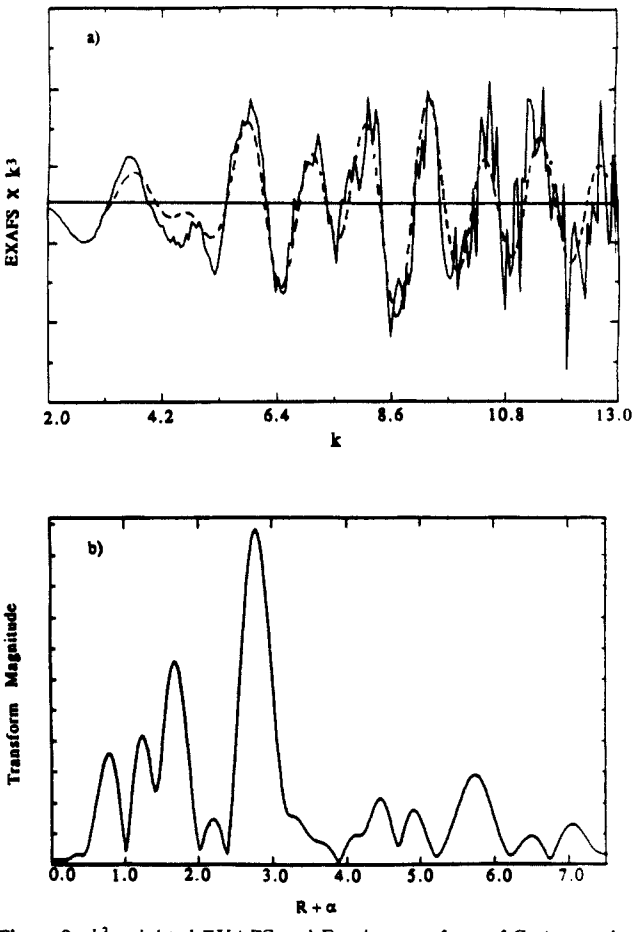

Figure 9. k^3 weighted EXAFS and Fourier transform of GaAs powder treated with pH = 12 (KOH) solution of 0.010 M $[Co^{II}(H_2O)_6](SO_4)$. X-ray fluorescence data collected on a focussed beam line at 77 K and 10^{-6} Torr. (a) Fluorescence EXAFS. Superimposed on the raw data is the fit (dashed curve) obtained from the summation of individual fits to the first-shell (Co–O) and second-shell (Co–Co) scattering contributions. (b) Fourier transform of a.

studies.[44] It also is consistent with the XPS and EXAFS data obtained in this work for the reaction of $[Co^{III}(NH_3)_5X]^{n+}$ (X = NH_3, OH_2, Br^-, N_3^-, OH^-) with GaAs single crystals and with GaAs powders.

The lack of reaction in 0.10 M HCl for both $[Co^{III}(NH_3)_5X]^{n+}$ (X = Br^-, OH_2) and $[Co^{III}(bpy)_3]^{3+}$ species indicates that the reduction potential of GaAs is a function of pH. This is expected from the Pourbaix diagrams for Ga and As.[33] Due to the irreversibility of the proposed reaction 1 above, we have not collected a full set of binding vs pH data to quantitatively estimate the formal redox potential for GaAs. However, it is clear that metal ions with reduction potentials positive of those for $[Co^{III}(NH_3)_5X]^{n+}$ (X = NH_3, Br^-, N_3^-, OH^-) and $[Co^{III}(bpy)_3]^{3+}$ (i.e.,

Table V. ^{57}Co Coverage on Single-Crystal GaAs

experiment[a]	CPM[b]	surface coverage[c]
H_2O background[d]	50 ± 2	
Pt background pH = 12.0 (KOH)	1123 ± 342[e]	
GaAs + $[^{57}Co^{III}(NH_3)_6]^{3+}$ pH = 12.0 (KOH)	104933	1.09×10^{-8}
	73612	7.6×10^{-9}
	81864	8.5×10^{-9}
average, base treatment (±1 standard deviation)	86803 ± 16234	$(9.0 \pm 1.7) \times 10^{-9}$
GaAs + $[^{57}Co^{III}(NH_3)_6]^{3+}$ pH = 12.0 (KOH), then immerse	75808	7.9×10^{-9}
	75163	7.8×10^{-9}
pH = 1.0 (HCl), 30 s[f]	68041	7.1×10^{-9}
average, base treatment followed by acid immersion[f] (±1 standard deviation)	73004 ± 4310	$(7.6 \pm 0.4) \times 10^{-9}$
Pt background, pH = 1.0 (HCl)[g]	148 ± 15	
GaAs + $[^{57}Co^{III}(NH_3)_6]^{3+}$ pH = 1.0 (HCl)	(−27 ± 23)[h]	*i*
	(−2 ± 24)[h]	*i*
	(−38 ± 22)[h]	*i*
average, pH = 1.0 treatment	(−22 ± 23)[h]	*i*

[a] 1 min exposure to 3.46 mM radiolabeled (^{57}Co) $[Co^{III}(NH_3)_6](Cl)_3$ solution at the pH indicated. [b] Counts per minute, foreground–Pt background for all entries except backgrounds. Calibration curve gives 9.16×10^{-14} mol(Co)/cpm. [c] Mol(Co)·cm^{-2} (GaAs), GaAs area = 0.884 cm^2. [d] Background obtained from deionized water. [e] GaAs samples were immersed in radiolabeled and etch solutions in a basket made from thin Pt wire. Counts observed from etched and rinsed Pt thread basket after immersion in pH = 12.0 ^{57}Co ammine solution. [f] Counts observed in acid immersion solution. [g] Counts observed from etched and rinsed Pt thread basket after immersion in pH = 1.0 ^{57}Co ammine solution. [h] Foreground–Pt background including ±1 standard deviation. [i] Negative cpm indicates Co coverage, if any, well below detectability limit. Foreground count rate places an upper limit $< 1 \times 10^{-11}$ mol(Co)·cm^{-2} on GaAs, i.e. <1/100th of a monolayer.

(44) (a) Frese, K. W., Jr.; Madou, M.; Morrison, S. R. *J. Phys. Chem.* **1980**, *84*, 3172. (b) Frese, K. W., Jr.; Madou, M.; Morrison, S. *J. Electrochem. Soc.* **1981**, *128*, 1527. (c) Frese, K. W., Jr.; Madou, M.; Morrison, S. *J. Electrochem. Soc.* **1981**, *128*, 1939.

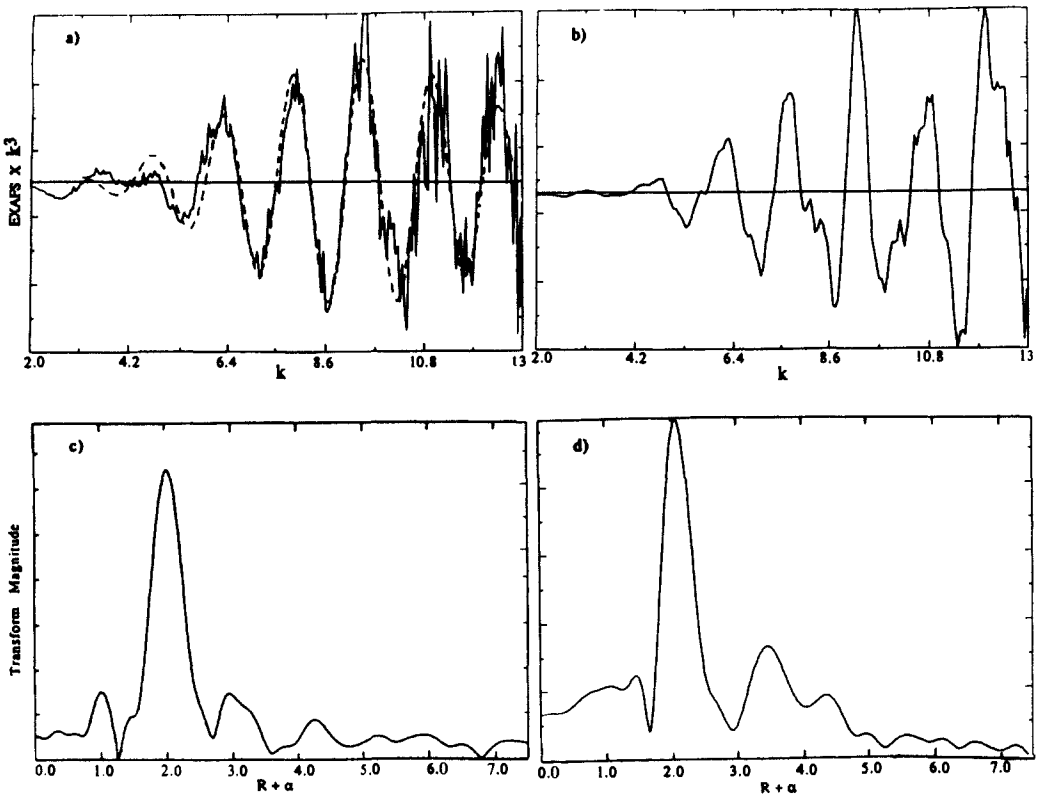

Figure 10. k^3 weighted EXAFS and Fourier transform data of $CoSe_2$ model compound and of GaAs powder initially treated with a pH = 12 (KOH) solution of 0.010 M $[Co^{III}(NH_3)_6]^{3+}$ and subsequently exposed to 1.0 M KOH–0.8 M K_2Se–0.1 M K_2Se_2 electrolyte. Model compound data were collected in the X-ray transmission mode, and GaAs powder data were collected in the fluorescence mode; both sets were obtained on a focussed beam line at 77 K and 10^{-6} Torr. (a) Fluorescence EXAFS of $KOH_{(aq)}$-$Se^{-/2-}$ exposed Co-treated GaAs powder. Superimposed on the raw data is the fit (dashed curve) obtained from the first-shell (Co–Se) scattering contribution. (b) Transmission EXAFS of the $CoSe_2$ model compound. (c) Fourier transform of a. (d) Fourier transform of b.

$E^{\circ\prime} > +0.2$ V vs SCE) can be expected to be reduced by GaAs at pH >10. Furthermore, more oxidizing species, such as Fe^{3+}, will be reduced by GaAs at lower pH values, as was observed in this work.

The measurable binding of $Co(OH)_2$ from aqueous 0.010 M KOH solutions of Co^{2+} is consistent with the formation of an arrested precipitate of the insoluble $Co(OH)_2$ on the GaAs surface.[42] The surface accumulation of $Co(OH)_2$ is expected to be far greater when it is formed at pH >10 (where $Co(OH)_2$ is insoluble) from the reduction of Co(III) ammines by the GaAs surface, and this is confirmed by the quantitative coverage data presented above. Although the overlayer obtained either from reactions of Co^{II} or $[Co^{III}(NH_3)_5X]^{n+}$ (X = NH_3, Br^-, N_3^-, OH^-) with GaAs was found to contain Ga, As, and Co, the close similarity of the first- and second-shell EXAFS data to that of $Co(OH)_2$ strongly suggests that most of the adsorbed Co from these precursors is in the $Co(OH)_2$ structure and stoichiometry.

One of the key issues in surface passivation studies is the chemical nature of electrical trap sites.[45] Prior work with Ru^{3+} chemisorption has described reductions in the GaAs surface recombination velocity at air interfaces,[46] as well as improvements in current–voltage behavior at semiconductor/liquid junctions.[4,47] Due to the relatively high coverage of Co (3–10 monolayers) and the similarity in X-ray scattering factors between Co, Ga, and As, our studies have been unable to identify the GaAs surface moiety that is responsible for binding Co. However, recent electrochemical studies have shown that the predominant effect of metal ion binding on GaAs is to increase the interfacial charge-transfer rate in the KOH-$Se^{-/2-}$ electrolyte[8b,9,18b,c] as opposed to decreasing the surface recombination rates, so chemical studies of variation in the electrical trap levels at this GaAs surface are not expected to have direct relevance to the reported photoelectrochemical properties of the GaAs surface. It would be of general interest to identify the various important ligation properties of the GaAs surface toward metal ions, and studies with $[Ru^{II}(NH_3)_5(OH_2)]^{2+}$ and other suitable complexes are currently being pursued to attain this goal.

The studies in this work also show that metal ion binding alone may not be sufficient to improve the electrical behavior of a semiconductor/liquid interface. The XPS and EXAFS studies of Co chemisorption clearly indicate that reactions of the surface-bound metal ion with the KOH-$Se^{-/2-}$ electrolyte yield the species of photoelectrochemical interest. We have previously shown that treatment of GaAs with $[Co^{III}(NH_3)_5X]^{n+}$ (X = NH_3, Br^-, N_3^-, OH^-) complexes does not result in a substantial reduction of the surface recombination velocity at air interfaces,[8a] yet the chemical change in the KOH-$Se^{-/2-}$ electrolyte does result in an improved current–voltage characteristic of the n-GaAs/KOH-$Se^{-/2-}$ junction.[8a,18] Thus, correlations between reactivity and electrical properties must account for possible chemical reactions that can create the surface species of electrical interest. An important consequence of the redox activity of the GaAs semiconductor surface is that the dissolved metal ions used for surface treatment might serve merely as precursors for the oxidation state that is actually bound on the semiconductor surface. This appears to be relevant to previous studies of metal ion binding on GaAs[2,4,8a,9,18] and should also be considered in explaining the pH dependence of metal ion binding for ions at GaAs surfaces. Similar considerations have been noted in studies of the behavior of gold ion adsorption on the natural mineral semiconductors PbS and FeS_x ($1 \le x \le 2$).[48] This would also seem to be relevant

(45) Many, A.; Goldstein, Y.; Grover, N. B. *Semiconductor Surfaces*; North Holland: Amsterdam, 1965.

(46) (a) Nelson, R. J.; Williams, J. S.; Leamy, H. J.; Miller, B.; Parkinson, B. A.; Heller, A. *Appl. Phys. Lett.* **1980**, *36*, 76. (b) Gmitter, T. J.; Yablonovitch, E.; Heller, A. *J. Electrochem. Soc.* **1988**, *135*, 2391.

(47) (a) Heller, A. *Acc. Chem. Res.* **1981**, *14*, 154. (b) Hodes, G.; Fonash, S. J.; Heller, A.; Miller, B. *Adv. Electrochem. Electrochem. Eng.* **1984**, *13*, 113.

(48) Jean, G. E.; Bancroft, G. M. *Geochim. Cosmochim. Acta* **1985**, *49*, 979.

to efforts to characterize the photoelectrochemical effect of Ru^{3+} on GaAs by investigating changes in the interface trap density of GaAs that has been exposed to Ru^0 in ultra-high-vacuum,[49] and to the general usefulness of the Ru^{3+} ion as a surface passivant when in contact with air,[46] aqueous I^-/I_3^-,[50] and other potentially reactive interfaces.[51]

In summary, the interfacial reactions of Co(III) and Co(II) complexes with GaAs surfaces have been identified, and the structure of the surface-bound species has been identified by a combination of methods. Other metal ions may employ different modes of binding to chemisorb on GaAs surfaces, and a complete set of spectroscopic studies would be needed in order to elucidate the chemical state of the various other surface treatments that have been identified in the literature. Such studies would be especially important for ions that can drastically change the rate of surface recombination under high-level-injection conditions (implying a reduction in surface state trapping rates as opposed to a chemisorption-induced shift in surface potential), although no such metal ion systems have yet been identified in the literature. We have also shown that the initial metal binding state need not be representative of the species relevant to the electrical behavior of semiconductor electrodes and that in situ characterization methods are required in order to address these issues. Ongoing efforts to discover suitable systems for surface passivation, and to characterize the chemical state of these surfaces, are continuing in this laboratory.

Acknowledgment. We thank the Department of Energy, Office of Basic Energy Sciences, for support of this work; the Stanford Synchrotron Radiation Laboratory, which is operated by the Department of Energy, Division of Chemical Sciences, for synchrotron facilities; the SSRL Biotechnology Program, supported by the National Institutes of Health, Biomedical Resource Technology Program, Division of Research Resources, for the loan of equipment used in EXAFS studies; and the National Science Foundation for support of XPS facilities maintained by the Center for Material Research at Stanford University. We gratefully acknowledge Dr. Britt M. Hedman of SSRL for assistance with EXAFS experiments and for helpful discussions. We thank Dr. C. L. R. Lewis of Varian Associates, Palo Alto, CA, for a generous supply of GaAs samples, Professors W. Huestis and H. McConnell of Stanford University for the use of scintillation and gamma counting instrumentation, Professor G. Brown of Stanford University for providing an authentic sample of Skutterudite, Professor M. Hochella, Jr., of Stanford University for help maintaining the X-ray photoelectron spectrometer, access to powder X-ray diffractometers and useful discussions, and M. Heben, A. Kumar, Dr. R. Penner, G. Ryba, M. Schmidt, and the SSRL staff for general assistance with the EXAFS experiments. S.R.L. acknowledges the Department of Education for a Fellowship, and N.S.L. acknowledges support as a Dreyfus Teacher-Scholar.

(49) Ludwig, M.; Heymann, G.; Janietz, P. *J. Vac. Sci. Technol.* **1986**, *B4*, 485.
(50) Allongue, P.; Cachet, H.; Clechet, P.; Froment, M.; Martin, J. R.; Verney, E. *J. Electrochem. Soc.* **1986**, *209*, 219.
(51) Mandel, K. C.; Basu, S.; Bose, D. N. *J. Phys. Chem.* **1987**, *91*, 4011.

Theoretical Study of Potential Wells and Barriers for S_N2 Rearrangement in the Systems $(XCH_3X)^-$ with X = F, Cl, and Br

Reinhard Vetter and Lutz Zülicke*

Contribution from the Central Institute of Physical Chemistry, Academy of Sciences of the GDR, Berlin DDR-1199, GDR. *Received September 11, 1989. Revised Manuscript Received January 25, 1990*

Abstract: Potential energy characteristics (well depths and barrier heights) for S_N2 rearrangement of the three symmetrical systems $(XCH_3X)^-$ with X = F, Cl, and Br have been calculated by using quantum chemical configuration interaction (CI) approaches with extended basis sets. The ion–dipole complex stabilities are found to be 11–13 kcal/mol for X = F and 8–9 kcal/mol for X = Cl and Br. The barrier heights (relative to the energy of the separate reactants) are obtained as 1–3 kcal/mol for X = F and Br but 7–8 kcal/mol for X = Cl. These results show some unexpected features; at present, they cannot be conclusively compared with experimental data. Therefore, our study should stimulate, on the one hand, further experimental investigations together with careful analysis of the measured quantities and, on the other hand, further refined quantum chemical treatments.

I. Introduction

Bimolecular nucleophilic substitution (S_N2) is an important reaction type of organic chemistry that has been the subject of extensive studies for many years. Experimental results on these reactions in solution[1a-c] revealed a number of regularities relating the reactivity to the nature and structure of the nucleophile, the leaving group, and the substrate. These findings, however, are strongly dependent on the solvent, and no unambiguous information can be obtained from this source about the "genuine" molecular mechanism. This became only possible in the early 1970s when experimentalists succeeded in studying these reactions in the gas phase. Most research work of this kind has been done on simple prototype S_N2 reactions

$$X^- + CH_3Y \rightarrow XCH_3 + Y^- \qquad (1)$$

by Bohme et al.,[2a-e] Brauman et al.,[2a,f-k] and more recently, DePuy

(1) (a) Ingold, C. K. *Structure and Mechanism in Organic Chemistry*; 2nd ed.; Cornell University Press: Ithaca, 1969. (b) Parker, A. J. *Chem. Rev.* **1969**, *69*, 1. (c) Harris, J. M., McManus, S. P., Eds. *Nucleophilicity*; Advances in Chemistry Series 215; American Chemical Society: Washington, DC, 1987.

0002-7863/90/1512-5136$02.50/0